Published in final edited form as:
Free Radic Biol Med. 2013 July ; 60: . doi:10.1016/j.freeradbiomed.2013.02.016.

Redox activation of Fe(III)-thiosemicarbazones and Fe(III)-bleomycin by thioredoxin reductase: specificity of enzymatic redox centers and analysis of reactive species formation by ESR spin trapping

Judith M. Myers[a,1], **Qing Cheng**[d,1], **William E. Antholine**[b,c], **Balaraman Kalyanaraman**[b,c], **Aleksandra Filipovska**[e], **ArnerElias S.J. Arnér**[d], and **Charles R. Myers**[a,c,*]

[a]Department of Pharmacology and Toxicology, Medical College of Wisconsin, Milwaukee, WI 53226, USA

[b]Department of Biophysics, Medical College of Wisconsin, Milwaukee, WI 53226, USA

[c]Free Radical Research Center, Medical College of Wisconsin, Milwaukee, WI 53226, USA

[d]Division of Biochemistry, Department of Medical Biochemistry and Biophysics, Karolinska Institutet, SE171 77 Stockholm, Sweden

[e]Western Australian Institute for Medical Research and Centre for Medical Research, The University of Western Australia, Perth, Australia

Abstract

Thiosemicarbazones such as triapine (Tp) and Dp44mT are tridentate iron (Fe) chelators that have well-documented anti-neoplastic activity. While Fe-thiosemicarbazones can undergo redox-cycling to generate reactive species that may have important roles in their cytotoxicity, there is only limited insight into specific cellular agents that can rapidly reduce Fe(III)-thiosemicarbazones and thereby promote their redox activity. Here we report that thioredoxin reductase-1 (TrxR1) and glutathione reductase (GR) have this activity, and that there is considerable specificity to the interactions between specific redox centers in these enzymes and different Fe(III) complexes. Site-directed variants of TrxR1 demonstrate that the selenocysteine (Sec) of the enzyme is not required, whereas the C59 residue and the flavin have important roles. While TrxR1 and GR have analogous C59/flavin motifs, TrxR is considerably faster than GR. For both enzymes, $Fe(III)(Tp)_2$ is reduced faster than $Fe(III)(Dp44mT)_2$. This reduction promotes redox cycling and the generation of hydroxyl radical ($HO^{\bullet}$) in a peroxide-dependent manner, even with low μM levels of $Fe(Tp)_2$. TrxR also reduces Fe(III)-bleomycin and this activity is Sec-dependent. TrxR cannot reduce Fe(III)-EDTA at significant rates. Our findings are the first to demonstrate pro-oxidant reductive activation of Fe(III)-based antitumor thiosemicarbazones by interactions with specific enzyme species. The marked elevation of TrxR in many tumors could contribute to the selective

*Corresponding author at: Dept. of Pharmacology and Toxicology, Medical College of Wisconsin, 8701 Watertown Plank Road, Milwaukee, WI 53226, USA. Tel.: +1-414 955 8593; fax: +1 414 456 6545. cmyers@mcw.edu.
[1]Both authors contributed equally to this work.

Conflict of interest
The authors do not have any conflict of interest.

tumor toxicity of these drugs by enhancing the redox activation of Fe(III)-thiosemicarbazones and the generation of reactive oxygen species such as $HO^{\bullet}$

Keywords

Triapine; Thiosemicarbazones; ESR; Hydroxyl radical; Thioredoxin reductase; Glutathione reductase; Bleomycin

1. Introduction

Thiosemicarbazones such as triapine (Tp) (3-aminopyridine-2-carboxaldehyde thiosemicarbazone) and Dp44mT (2,2′-Dipyridyl-N,N-dimethylsemicarbazone) are tridentate iron (Fe) chelators with pronounced antineoplastic activity [1]. Because Fe markedly prefers octahedral coordination geometries for both Fe(III) and Fe(II), two thiosemicarbazone molecules bind one Fe atom to complete the 6-coordination complex, e.g. $Fe(Tp)_2$ or $Fe(Dp44mT)_2$ [1–3]. The Fe in Fe-thiosemicarbazone complexes is redox active and can be redox-cycled [1, 4, 5]. Such cycling could generate reactive oxygen species (ROS) that are important for cytotoxicity. For example, thiosemicarbazones can lead to inhibition of ribonucleotide reductase (RR) in cells [1], but Tp or $Fe(III)(Tp)_2$ may not directly inhibit RR [5]. Recent studies with the purified R2 subunit of mouse RR show that the reduced form, $Fe(II)(Tp)_2$, damages RR in an O_2-dependent manner [6], suggesting that ROS generation from $Fe(II)(Tp)_2$ was responsible. This is consistent with the observation that the potent Fe chelator deferoxamine, which stabilizes Fe(III) and thereby prevents Fe redox cycling and ROS generation [4], protects cells from Tp [7]. Electron spin resonance (ESR) studies with the spin trap 5,5,-dimethyl-1-pyrroline *N*-oxide (DMPO) and the hydroxyl radical ($HO^{\bullet}$) scavenger dimethylsulfoxide (DMSO) are consistent with the generation of $HO^{\bullet}$ from Fe(II) plus Tp [5] or Dp44mT [8], likely by Fenton-like chemistry. Together, these results imply that the pro-oxidant effects of Fe-thiosemicarbazone complexes such as $Fe(Tp)_2$ are very important to the cytotoxic action. Consistent with this hypothesis, recent studies demonstrate that Tp causes significant cellular oxidative stress as reflected in the pronounced oxidation of endogenous redox-sensitive proteins such as mitochondrial thioredoxin-2 (Trx2) and peroxiredoxin-3 (Prx3) [9]. Since peroxiredoxins are very sensitive to oxidation by peroxide substrates [10], and since Prx3 oxidation in Tp-treated cells is not necessarily dependent on Trx2 oxidation [9], these findings suggest significant peroxide generation in Tp-treated cells. $Fe(Tp)_2$ redox cycling could also lead to the generation of other reactive oxygen species (ROS).

In order to maximize the cytotoxicity of antitumor Fe(III) complexes such as the Fe(III)-thiosemicarbazones, it is important to understand in detail the mechanisms that support their efficient redox cycling. However, specific cellular mechanisms that support their redox activation are not well defined. In vitro studies have shown that cysteine (Cys) or reduced glutathione (GSH) can reduce $Fe(III)(Tp)_2$ to $Fe(II)(Tp)_2$, but Cys is ~4-fold faster and significantly more efficient than GSH [9]. This is consistent with the pK_a values of their thiols (8.3 for Cys, 8.9 for GSH). However, the concentration of free Cys in cells is rather low (<0.1 mM) [11, 12]. While GSH is the most abundant low molecular weight thiol in cells (1–11 mM), the concentration of total protein thiols is much greater than that of GSH [13]. However, there is little known about the ability of protein thiols or of other protein redox-active centers to reduce Fe(III)-thiosemicarbazones. We therefore sought to identify cellular proteins that can reduce Fe(III)-thiosemicarbazones at high rates. A diverse array of cancer cells are sensitive to the thiosemicarbazones [14–19], and cancer cells are typically more sensitive to thiosemicarbazones than normal cells [20]. Therefore, redox enzymes that can reductively activate Fe(III)-thiosemicarbazones and that are overexpressed in cancer

cells could contribute to this drug sensitivity. Proteins with a variety of redox centers, such as thioredoxin reductase (TrxR), could have a higher probability of reducing Fe(III) complexes. Mammalian cytosolic TrxR1 is expressed in all cells, is markedly overexpressed in many cancers [21–23], and it can reduce a variety of substrates including thioredoxins, selenite, dehydroascorbate, lipid hydroperoxides, α-lipoic acid, and disulfides in some other proteins [24–26]. TrxR1 has three different types of redox centers, with each homodimer subunit containing one flavin (FAD) that accepts electrons from NADPH, an N-terminal domain dithiol (-CVNVGC- whose Cys residues occupy positions C59/C64 in TrxR1 studied here) that is reduced by the flavin, and a C-terminal domain that contains Cys and selenocysteine (Sec) within the sequence -Gly-Cys-Sec-Gly [27–30]. The Cys-Sec (C497/U498) active site, which is believed to accept electrons from the N-terminal dithiol, is essential for the reduction of oxidized thioredoxins, and plays a major role in the reduction of artificial disulfide substrates such as 5,5′-dithiobis(2-nitrobenzoic) acid (DTNB) [31]. When TrxR is reduced by NADPH, the nucleophilic and highly reactive reduced Sec residue becomes surface-exposed and is prone to react with substrates or inhibitors [25, 27, 28, 32–35]. However, some substrates (e.g. selenocystine, selenite, lipoic acid) and inhibitors (e.g. aurothioglucose) are not solely dependent on the Sec and may alternatively interact with the C59/C64 dithiol, at least for the mitochondrial isoenzyme TrxR2 [36]. The N-terminal flavin and C59/C64 dithiol domains of TrxR resemble those in glutathione reductase (GR), but only TrxR has the C-terminal Cys-Sec motif.

We herein present an in-depth investigation of the reductive activation of Fe(III)$(Tp)_2$ and Fe(III)$(Dp44mT)_2$ by TrxR1 and GR, and the resulting generation of multiple reactive species. TrxR1, in particular, has high activity with the Fe(III)-thiosemicarbazones. A series of site-directed variants of TrxR were used to characterize the role of its various redox centers, and revealed that there is considerable specificity to the redox interactions between the TrxR redox centers and different Fe(III) complexes. TrxR could have an important role in enhancing the pro-oxidant effects of Fe(III)-based antitumor agents for which Fe(III) reduction is critical to their cytotoxic effects. To our knowledge, this is also the first demonstration of the ability of mammalian TrxR1 to reduce Fe(III) complexes.

2. Materials and methods

2.1. Reagents

Tp was kindly provided by Vion Pharmaceuticals, and stock solutions were prepared in 95% acetonitrile. Fe(III)$(Tp)_2$ was generated by mixing 2 volumes of 5 mM Tp with 1 volume of freshly prepared 5 mM aqueous $FeCl_3$, followed by 1 h incubation at 37°C. Dp44mT (2,2′-Dipyridyl-N,N-dimethylsemicarbazone) was obtained from Calbiochem, and was protected from light. Stock solutions of Dp44mT were prepared in 95% acetonitrile. Fe(III)$(Dp44mT)_2$ was generated by mixing 2 volumes of 5 mM Dp44mT with 1 volume of freshly prepared aqueous 5 mM $FeCl_3$, followed by 1 h incubation at 37°C. Fe(III)-EDTA was prepared with excess EDTA by mixing 2 volumes of 5 mM EDTA (pH 8) with one volume of freshly prepared 5 mM $FeCl_3$, followed by 1 h incubation at 37°C. These Fe(III) complexes were held at 4°C until use.

Bleomycin (Blm) was purchased from Santa Cruz Biotechnology (Santa Cruz, CA), and was protected from light. Stock solutions were prepared in 10 mM Tris-HCl pH 7.5. Fe(III)-Blm was prepared by mixing a 5% molar excess of Blm with ferrous ammonium sulfate (prepared immediately before use in anaerobic water). After 15 min incubation at room temperature under room air, the Fe(III)-Blm was held at 4°C until use.

The visible absorbance spectra (335–700 nm) of these Fe(III) complexes and their reduced Fe(II) forms (generated by reduction with dithiotheitol or sodium dithionite) were consistent with published spectra.

The spin trap 5-diethoxyphosphoryl-5-methyl-1-pyrroline-*N*-oxide (DEPMPO) was obtained from Radical Vision (Marseille, France). The spin trap α-phenyl-*N*-*tert*-butylnitrone (PBN) was from Alexis Biochemicals (Lausen, Switzerland). Ferrous ammonium sulfate and H_2O_2 were from Mallinckrodt Chemicals (Phillipsburg, NJ). Superoxide dismutase (SOD) was from Sigma (cat. no. S5395, from bovine erythrocytes), and catalase was from Calbiochem (cat. no. 219001, from bovine liver). Tris was obtained from Research Organics (Cleveland, OH), and EDTA was from Fisher Scientific (Hampton, NH). Dimethylsulfoxide (DMSO) and all other chemicals and reagents were purchased from Sigma-Aldrich (St. Louis, MO).

2.2 Recombinant TrxR1 and site-directed variants, and other enzymes

Wild-type rat TrxR1 (wtTrxR1) and the site-directed TrxR1 variants were generated and purified from recombinant systems as previously described [27, 37–41]. Variants lacking the active site Sec (U498) include U498C and a truncated variant that is missing U498 and G499. Variants affecting the N-terminal domain dithiol include C59S, C64S, and C59S/C64S. Additional details regarding the recombinant TrxR preparations are included in the Supplement. The concentration of each TrxR variant was determined spectrophotometrically using the molar extinction coefficient of FAD (13600 $M^{-1}cm^{-1}$ at 463 nm) assuming one FAD per subunit. Concentrations of TrxR in the experiments refer to concentration of the dimer, which is the active form of TrxR. The kinetic parameters of wtTrxR and its variants with the disulfide substrate DTNB were reported previously [41].

Human Trx2 (amino acids 59–166) was generated and purified from a recombinant system as described by Rackham et al. [42]. Purified yeast GR (from Sigma) was supplied as a suspension in ammonium sulfate, and was dialyzed overnight at 4°C against Chelex-treated 50 mM phosphate buffer, pH 7.35. The activity of the dialyzed GR was verified by the stimulation of NADPH consumption upon the addition of glutathione disulfide (GSSG) [43].

2.3 General procedures

To remove polyvalent trace metal ion contaminants, aqueous solutions were pretreated with Chelex-100 (4% w/v) for >12 h before use. Experiments under aerobic conditions were conducted under room air. Anaerobic conditions were established in an anaerobic chamber (Coy Laboratory Products, Grass Lake, MI) (4 to 5% H_2, balance N_2) as previously described [44]. Buffers and deionized water were pre-incubated in the anaerobic chamber for ≥24 h before use.

2.4 Electron Spin Resonance (ESR)

Species with an unpaired electron, including reactive oxygen species and carbon-centered radicals, were assessed at fixed time points using ESR spin trapping as described previously [41, 45]. Aqueous solutions were pre-treated with Chelex-100 resin for >12 h prior to use. The buffer (final concentration in assay of 0.15 M KCl/12.5 mM potassium phosphate pH 7.4) and water were pre-warmed to 37°C. NADPH (0.4 mM), TrxR (0.3 μM), DEPMPO (14 mM), and Fe(III) complexes (final concentrations as indicated in the Results) were added and incubation was continued for 15 min. In some experiments, Tp or Dp44mT were substituted as controls for $Fe(Tp)_2$ or $Fe(Dp44mT)_2$.Where indicated, 250 mM ammonium formate was included as a $HO^{\bullet}$ scavenger. In some experiments, the spin trap PBN (50 mM) plus 5% DMSO (v/v) were substituted for DEPMPO. The reactions were stopped by immersion in liquid nitrogen (77 K), and were stored in liquid nitrogen until analysis by ESR. Freezing and thawing does not change the ESR spectra of DEPMPO adducts [46, 47].

For ESR spin trapping analysis, samples were quickly thawed, placed in a quartz flat cell and ESR spectra were obtained without delay at room temperature using a Bruker EMX spectrometer. Instrument settings are indicated in the results. ESR spectra were confirmed in replicate experiments. The hyperfine couplings were measured from the ESR data, and were confirmed using the simulation software WinSim (version 0.95) (National Institutes of Environmental Health Sciences) [48]. The concentration of each species was obtained by double integration of the simulated spectra using WinSim software. 4-hydroxy-2,2,6,6-tetramethylpiperidine 1-oxyl was used as the standard.

In some experiments, ESR was used to follow the loss of the Fe(III) signal. In these experiments, the reactions were transferred to 4-mm quartz ESR tubes, immersed in liquid nitrogen (77 K) and stored, typically for less than one week. ESR spectra were obtained at 37 K using a Bruker E500 ELEXSYS spectrometer (Silberstreifen, Germany) with an Oxford Instruments ESR-9 helium flow cryostat (Oxfordshire, UK) and a Bruker DM0101 cavity.

2.5 Rates of reduction of Fe(III) complexes

The buffers and reagents were the same as those described for ESR spin trapping (above), except that DEPMPO was not included. For experiments with $Fe(Tp)_2$ and $Fe(Dp44mT)_2$, the final enzyme concentration (TrxR variants or GR) was reduced to 0.03 μM to facilitate accurate assessment of the initial rates. The buffer and water were pre-warmed to 37°C in semi-micro cuvettes, and then NADPH (0.4 mM), TrxR (0.03 μM), and $Fe(III)(Tp)_2$ or $Fe(III)(Dp44mT)_2$ were added (final concentrations as indicated in the Results). The reduction to the corresponding Fe(II) forms was followed over time at 610 nm for $Fe(II)(Tp)_2$, and at 623 nm for $Fe(II)(Dp44mT)_2$, which are absorbance peaks specific to the Fe(II) forms. The initial rates of reduction were used for the calculations. Controls included the substitution of Tp or Dp44mT for $Fe(III)(Tp)_2$ or $Fe(III)(Dp44mT)_2$, and testing NADPH without enzyme.

Since there are not absorbance differences between Fe(III)-Blm and Fe(II)-Blm of sufficient intensity for these rate experiments, the bathophenanthroline disulfonate (BPS) method was used to measure the rate of Fe(III)-Blm reduction [49]. BPS reacts very quickly with Fe(II)-Blm to form the $Fe(II)(BPS)_3$ complex which has intense absorbance at 534 nm (extinction coefficient of 22.14 mM^{-1} cm^{-1}) [49]. The conditions were the same as for the Fe-thiosemicarbazone rate experiments, except that the final concentration of wtTrxR was 0.3 μM, and 1 mM BPS was included. The rates were compared to Fe(III)-Blm with NADPH or without a reductant. Positive controls included 0.2 mM ascorbic acid or cysteine, which are known chemical reductants of Fe(III)-Blm [49, 50].

2.6 Statistical analysis

Statistical analysis of three or more groups of data were done using one-way ANOVA and the Tukey-Kramer post test (Prism software, Graphpad). Significance was assumed at $P < 0.05$.

3. Results

3.1 Spin trapping of radicals formed by the reductive activation of $Fe(Tp)_2$

The spin trap DEPMPO was used to follow the generation of various radicals during the aerobic incubation of $Fe(III)(Tp)_2$ with Cys, GSH, or TrxR plus NADPH (Fig. 1). DEPMPO is well-suited for these studies. It allows for simultaneous analysis of $O_2^{\bullet -}$, $HO^{\bullet}$, and thiyl and carbon radical adducts, and DEPMPO/$HOO^{\bullet}$ does not spontaneously decay to DEPMPO/$HO^{\bullet}$ [46, 51]. Furthermore, the high oxidation potential of DEPMPO (2240 mV

vs. NHE) [52] makes it unreactive with other strong oxidants such as singlet oxygen [53]. Also, even in the presence of 1 mM Fe(II), there is no spontaneous formation of DEPMPO/$HO^{\bullet}$ in phosphate buffered systems [46].

While the ESR signals generated with Cys and GSH as reductants of $Fe(III)(Tp)_2$ appear small relative to the other signals shown, the species present were clearly defined by the simulation software. With 5 mM Cys, the predominant signal was that of a thiyl radical adduct (a^P = 45.8 G, a^H = 14.9 G, a^N = 14.1 G) with smaller contributions for the $HO^{\bullet}$ (17%) (a^P = 47.1 G, a^H = 13.2 G, a^N = 14.1 G) and $O_2^{\bullet -}$ adducts (14%) (a^P = 49.97 G, a^H = 10.98 G, a^N = 13.2 G) of DEPMPO (Fig. 1a). With 1 mM Cys, the signal was smaller and the predominant component was DEPMPO/$HO^{\bullet}$ (63%) with the remainder due to the $O_2^{\bullet -}$ (24%) and thiyl radical adducts (13%) (Fig. 1b). DEPMPO adducts were minimal with 5 mM GSH as the reductant (Fig. 1c), whereas the signal with 1 mM GSH was predominantly DEPMPO/$HO^{\bullet}$ (63%) with the rest attributed to the $O_2^{\bullet -}$ (23%) and thiyl radical adducts (14%) (Fig. 1d). The signal for $Fe(III)(Tp)_2$ without reductant (Fig. 1e) was minimal and did not have a distinct pattern.

Compared to Cys and GSH, wild-type TrxR1 generated very robust spin adduct signals when incubated with 50 μM $Fe(III)(Tp)_2$ (Fig. 1f). The predominant signals were those of DEPMPO/$HO^{\bullet}$ (61%), and a 12-line signal for a carbon radical adduct (38%). When exogenous H_2O_2 (50 μM) was included, the $HO^{\bullet}$ and carbon radical adducts were 60% and 50% larger, respectively, with a very similar relative abundance of the two adducts (63 and 36%, respectively) (Fig. 1g). As reported previously [41], in the absence of $Fe(III)(Tp)_2$, wtTrxR generates a signal which is a mix of the $HO^{\bullet}$ and $O_2^{\bullet -}$ adducts (Fig. 1h). This results from its NADPH oxidase activity which generates $O_2^{\bullet -}$, and the Sec of wtTrxR then reduces the resulting DEPMPO/$HOO^{\bullet}$ adduct to DEPMPO/$HO^{\bullet}$ [41]. Additional experiments presented below include Sec-deficient variants. Overall, the addition of 50 μM $Fe(III)(Tp)_2$ to wtTrxR increases the $HO^{\bullet}$ adduct signal by 7-fold and the carbon radical adduct signal by 26-fold (Fig. 1f vs. 1h), suggesting pronounced radical generation from $Fe(Tp)_2$ redox cycling.

Experiments with wtTrxR and varied concentrations of $Fe(III)(Tp)_2$ indicate that both $HO^{\bullet}$ and carbon radical adducts of DEPMPO are prominent with 50 and 100 μM $Fe(III)(Tp)_2$, but that the $HO^{\bullet}$ adduct predominates at 2.5–25 μM $Fe(III)(Tp)_2$ (Fig. 2). Only small signals for the carbon radical and $O_2^{\bullet -}$ adducts are seen at these lower $Fe(III)(Tp)_2$ concentrations. Thus, the carbon radical adduct increases markedly (3.2-fold) when $Fe(III)(Tp)_2$ is increased from 25 to 50 μM, whereas the $HO^{\bullet}$ adduct signal is a major component with all $Fe(III)(Tp)_2$ concentrations and increases only 30% when $Fe(Tp)_2$ is increased from 25 to 50 μM. The relationship between the concentration of $Fe(Tp)_2$ and the amount of each DEPMPO adduct is shown in Supplemental Fig. S1.

The hyperfine coupling constants for the carbon radical adduct (Fig. 1 legend) closely resemble those for other low molecular weight carbon radicals such as the ethanol radical, but this signal was not due to radical reactions with the solvent. The triapine stock was prepared in acetonitrile (to avoid ethanol or DMSO, which have well-recognized reactions with $HO^{\bullet}$). Acetonitrile is very unreactive with oxygen-centered radicals including $HO^{\bullet}$ [54]. We confirmed that the Fenton reaction (0.15 mM ferrous iron plus 1.7 mM H_2O_2) in buffer containing DEPMPO plus 2% acetonitrile yields the DEPMPO/$HO^{\bullet}$ adduct, whereas the same reaction in 2% ethanol generates a 12-line signal consistent with the ethanol radical adduct (not shown).

Formate is oxidized by $HO^{\bullet}$ to yield a carbon dioxide radical anion which can be trapped as DEPMPO/$CO_2^{\bullet -}$ [55]. When formate was included with wtTrxR and 50 μM $Fe(III)(Tp)_2$,

both the $HO^{\bullet}$ and carbon radical adduct signals were essentially absent, and there was an intense signal matching that of DEPMPO/$CO_2^{\bullet -}$ (a^P = 51.6 G, a^H = 17.3 G, a^N = 14.5 G) (Fig. 2i). These formate data support the generation of $HO^{\bullet}$ from the redox cycling of $Fe(Tp)_2$, and imply that the carbon radical adduct formation is dependent on $HO^{\bullet}$.

The secondary radical trapping technique with α-phenyl-*N*-*tert*-butylnitrone (PBN) as the spin trap and dimethylsulfoxide (DMSO) as a $HO^{\bullet}$ scavenger further confirmed the generation of free $HO^{\bullet}$ by the TrxR-mediated redox cycling of $Fe(III)(Tp)_2$ (Supplemental Fig. S2).

Since the Fig. 2 data imply that higher $Fe(Tp)_2$ concentrations facilitate generation of the carbon radical, we tested whether elevated concentrations of Tp could similarly enhance carbon radical formation (Fig. 3). Both carbon radical and $HO^{\bullet}$ adducts are predominant with wtTrxR and 50 μM $Fe(Tp)_2$ (Fig. 3a), whereas the $HO^{\bullet}$ adduct is the predominant signal with 25 μM $Fe(Tp)_2$ (Fig. 3d) even when 50 or 100 μM excess Tp is included (Fig. 3b, c). Thus, while the carbon radical adduct is facilitated by higher levels of $Fe(Tp)_2$, the addition of excess free Tp does not similarly enhance carbon radical formation, nor does it alter the intensity of the DEPMPO/$HO^{\bullet}$ signal (Fig. 3b–d). To further confirm this, $Fe(III)(Tp)_2$ was also made with a 50% molar excess of Tp (referred to as $Fe(Tp)_{2+1}$), and allowed to incubate for 2.5 h before use to provide more than ample opportunity for all Fe to be bound to Tp. The ESR signals were the same for wtTrxR with $Fe(III)(Tp)_2$ vs. $Fe(III)(Tp)_{2+1}$ (not shown). These experiments demonstrate that the $HO^{\bullet}$ and carbon radicals are not generated from reactions involving free Fe.

While the identity of the carbon-based radical is not known, it is very unlikely that it is a TrxR radical because: (1) its symmetrical 12-line signal is consistent with that of a low molecular mass species, and not with TrxR (~112,000 Daltons for the homodimer), and (2) the carbon radical adduct was in ~6-fold molar excess relative to TrxR. The dependence of this carbon radical on $HO^{\bullet}$ (Fig. 2i) raises the possibility that it could result from $HO^{\bullet}$ attack on NADP(H) or $Fe(Tp)_2$. However, we were unable to see a similar 12-line signal when NADPH or $NADP^+$ (0.4–1.6 mM) or $Fe(Tp)_2$ (50 or 100 μM) were included with the Fenton reaction (0.60 mM ferrous iron plus 1.7 mM H_2O_2) (Supplemental Fig. S3), even though levels of DEPMPO/$HO^{\bullet}$ were 2.5- to 3.5-fold greater than those generated with TrxR in the presence of 50 or 100 μM $Fe(Tp)_2$. Thus, there should have been more than enough $HO^{\bullet}$ to theoretically generate a carbon radical from NADP(H) or $Fe(Tp)_2$. Together, the data suggest that there could be something unique about the redox interactions between TrxR and $Fe(Tp)_2$ that facilitates the generation of the carbon-based radical. This particular radical may not be generated at high levels in cells, however, as the large number of cell components available for reaction with $HO^{\bullet}$ could lead to a diverse array of secondary radicals. This carbon radical was not reported by other groups who did ESR experiments with the spin trap DMPO and dithiothreitol-reduced $Fe(Tp)_2$ [5] or with Fe(II) plus Dp44mT [8]. However, these studies used DMSO as a $HO^{\bullet}$ scavenger, thereby generating $^{\bullet}CH_3$ which was trapped by DMPO. This approach precluded the ability to determine if other DMPO/carbon radical adducts with similar hyperfine constants may have been formed.

Most of the remaining experiments were conducted with 50 μM $Fe(Tp)_2$ because it is the lowest concentration that generates significant levels of both $HO^{\bullet}$ and carbon radical adducts.

3.2 Reduction of $Fe(III)(Tp)_2$ by TrxR1 and the role of redox active centers within TrxR1

The chemical structures for Tp and $Fe(Tp)_2$ are shown in Fig. 4A, B. The pronounced stimulation of radical generation that occurs when $Fe(III)(Tp)_2$ is added to wtTrxR implies that TrxR efficiently reduces $Fe(III)(Tp)_2$ to $Fe(II)(Tp)_2$, a necessary step to support the

subsequent generation of radicals by redox cycling of the $Fe(Tp)_2$. To determine which redox centers of TrxR1 are necessary for $Fe(III)(Tp)_2$ reduction, we determined the rates at which wtTrxR and its various site-directed variants could reduce $Fe(III)(Tp)_2$. Since the reduced form, $Fe(II)(Tp)_2$, has greater absorbance at 340 nm than the oxidized form, NADPH oxidation cannot be followed at this wavelength as an indicator of Fe(III) reduction. Therefore, we followed the increase in absorbance at 610 nm, which is specific for the reduced Fe(II) form of $Fe(Tp)_2$ [9]. The initial rates were used to quantify $Fe(III)(Tp)_2$ reduction. Wild-type TrxR is very efficient at reducing $Fe(III)(Tp)_2$ (Fig. 4C). The truncated and U498C variants lack the Sec, but retain a functional flavin and C59/C64 dithiol, as shown earlier [31, 56]. These variants devoid of Sec were 1.5–2 times faster than wtTrxR (Fig. 4C) which suggests that the Sec is not required for $Fe(III)(Tp)_2$ reduction. While the C64S variant was marginally faster than wtTrxR, the rate of the C59S variant was 57% of that of wtTrxR1, and the C59S/C64S variant was even slower (only 31% of wtTrxR). While C59S and C64S variants retain the active site C-terminal C497/U498 residues, this C497/U498 site cannot be reduced and is therefore not functional. The flavin is the only recognized redox active domain in the C59S/C64S variant, so its rate of $Fe(III)(Tp)_2$ reduction likely represents direct reduction by the flavin. Together, the data indicate that the C59 and flavin are significant contributors to $Fe(III)(Tp)_2$ reduction, but that additional sites within TrxR may also contribute to the activity.

ESR was used to compare the radicals generated by wtTrxR1 and the truncated and C59S variants incubated with $Fe(III)(Tp)_2$ plus NADPH. There was no significant difference between the amounts of $HO^{\bullet}$, $O_2^{\bullet -}$ and carbon radical adducts generated by wtTrxR1 compared to the truncated (Sec-minus) variant (Fig. 5A, B). While the Sec is not required for $Fe(III)(Tp)_2$ reduction (Fig. 4C), the Sec was previously shown to be necessary to reduce DEPMPO/$HOO^{\bullet}$ to DEPMPO/$HO^{\bullet}$ [41]. The fact that wtTrxR and the truncated variant generate similar levels of DEPMPO/$HO^{\bullet}$ indicates that this signal primarily results from trapping of $HO^{\bullet}$, and not from the reduction of DEPMPO/$HOO^{\bullet}$. Compared with wtTrxR, C59S generates similar amounts of $O_2^{\bullet -}$ and carbon radical adducts, but lesser amounts of DEPMPO/$HO^{\bullet}$ (Fig. 5A, B). This lower $HO^{\bullet}$ generation may reflect the slower rate of $Fe(III)(Tp)_2$ reduction (Fig. 4C) catalyzed by C59S. As is the case for the truncated variant, C59S cannot reduce DEPMPO/$HOO^{\bullet}$ to DEPMPO/$HO^{\bullet}$, further supporting that its DEPMPO/$HO^{\bullet}$ signal results from trapping $HO^{\bullet}$. Unlike wtTrxR, C59S lacks significant NADPH oxidase activity, implying that the $O_2^{\bullet -}$ results from redox cycling of $Fe(Tp)_2$.

For all three of these TrxR variants, catalase markedly diminished the levels of $HO^{\bullet}$ and carbon radical adducts (Fig. 5A, C, D, E). This implies that both signals are largely H_2O_2-dependent. It further supports the hypothesis that the $HO^{\bullet}$ generated by TrxR largely results from Fenton-like reactions between $Fe(II)(Tp)_2$ and H_2O_2. The redox cycling of $Fe(Tp)_2$ likely generates $O_2^{\bullet -}$ which then dismutates to H_2O_2 to support $HO^{\bullet}$ generation. Although spin trapping with DEPMPO is a sensitive method for detecting $O_2^{\bullet -}$ [47], the DEPMPO/$HOO^{\bullet}$ signal never accounted for more than a small percentage of the total DEPMPO adducts seen in these experiments (Figs. 2, 5). It is possible that peroxide is also generated by alternative mechanisms. One possibility for peroxide generation from Fe(II)-thiosemicarbazones could be:

$$\mathrm{Fe(II)} + O_2 \rightarrow \mathrm{Fe(IV)} + H_2O_2. \quad (1)$$

However, in trial experiments we did not detect an EPR signal for Fe(IV). This does not exclude this possible mechanism, as Fe(IV) species have very high reactivity and thus very short half-lives. Nonetheless, cells have a number of additional mechanisms to promote

peroxide generation from the redox cycling of Fe-thiosemicarbazones, e.g. SOD rapidly converts $O_2^{\bullet -}$ to H_2O_2 (rate constant 1.4×10^9 M^{-1} s^{-1}).

The relatively small amount of DEPMPO/HO$^\bullet$ generated by wtTrxR in the presence of catalase (Fig. 5A, 5C) likely reflects its endogenous NADPH oxidase activity and the subsequent Sec-dependent reduction of DEPMPO/HOO$^\bullet$ to DEPMPO/HO$^\bullet$, as this mechanism was previously shown to be catalase-insensitive [41].

SOD diminished the small DEPMPO/HOO$^\bullet$ adduct signal as expected, but it did not change the levels of carbon radical adduct by any of the TrxR variants (Fig. 5C, D, E). While SOD caused some decrease in the intensity of the HO$^\bullet$ adducts generated by wtTrxR and truncated TrxR (Fig. 5C, D), these decreases were much less than those caused by catalase. The ability of SOD to partially decrease the DEPMPO/HO$^\bullet$ adducts generated by wtTrxR is consistent with the ability of wtTrxR to reduce DEPMPO/HOO$^\bullet$ to DEPMPO/HO$^\bullet$ [41], and implies that some of the HO$^\bullet$ signal generated by wtTrxR may be generated by this mechanism.

3.3 The redox activation of Fe(Dp44mT)$_2$ and Fe(III)-bleomycin by TrxR1

Dp44mT (see structure in Fig. 6A) is a thiosemicarbazone tridentate Fe chelator whose NNS ligands for Fe are analogous to Tp [20]. The ability of TrxR to reduce Fe(III)(Dp44mT)$_2$ was determined by following the increase in absorbance at 623 nm, which is specific for the reduced form, Fe(II)(Dp44mT)$_2$. TrxR1 reduced Fe(III)(Dp44mT)$_2$ (Fig. 6B), although the rates for most TrxR variants were 2- to 3.3-fold slower for Fe(III)(Dp44mT)$_2$ than for Fe(III)(Tp)$_2$ (Figs. 4C, 6B). The main exception was U498C, which was 5.9-fold slower at reducing Fe(III)(Dp44mT)$_2$ than Fe(III)(Tp)$_2$. While U498C had the fastest rate of reduction of Fe(III)(Tp)$_2$ (Fig. 4C), its reduction of Fe(III)(Dp44mT)$_2$ was similar to that of wtTrxR (Fig. 6B). Despite the slower rates of Fe(III)(Dp44mT)$_2$ reduction, similar redox centers within TrxR were important for both Fe(III)-thiosemicarbazones. Neither the Sec or C64 were required, whereas the C59 and flavin were important for the reduction of Fe(III)(Tp)$_2$ and Fe(III)(Dp44mT)$_2$ (Figs. 4C, 6B).

Consistent with the slower rates of Fe(Dp44mT)$_2$ reduction, the ESR spin adduct signals were significantly smaller with Fe(Dp44mT)$_2$ than with Fe(Tp)$_2$ for both wtTrxR and the truncated TrxR variant (Supplemental Fig. S5). The predominant signal with Fe(Dp44mT)$_2$ was DEPMPO/HO$^\bullet$, with lesser amounts of DEPMPO/HOO$^\bullet$, and only trace amounts of the 12-line carbon radical adduct signal. Fe(III)(Dp44mT)$_2$ also caused markedly slower O_2 consumption rates relative to Fe(III)(Tp)$_2$ (Supplemental Fig. S6).

Since this is the first report of the reduction of Fe(III) complexes by TrxR, we determined if wtTrxR could reduce other Fe(III) species, specifically Fe(III)-Blm and Fe(III)-EDTA. Since their reduced Fe(II) forms have increased absorbance at 340 nm, other methods were used to assess Fe(III) reduction. For Fe(III)-EDTA, we used (a) ESR at 37 K to follow the loss of the Fe(III) signals, and (b) O_2 consumption as an indicator of Fe-EDTA redox cycling. TrxR showed no ability to reduce Fe(III)-EDTA at significant rates: (a) there was no decline in the intensity of the Fe(III)-EDTA ESR signal (measured at 37 K) over 20 min (Supplemental Fig. S7A), and (b) Fe(III)-EDTA did not enhance O_2 consumption by wtTrxR (not shown). In contrast, wtTrxR decreased the ESR signal intensity of Fe(III)(Tp)$_2$ (Supplemental Fig. S7B) consistent with its ability to reduce Fe(III)(Tp)$_2$ to Fe(II)(Tp)$_2$, and thereby promote cycling between these two redox states. In contrast to Fe(III)-EDTA, wtTrxR does reduce Fe(III)-Blm (Fig. 7A, B). While the absolute rate of reduction of Fe(III)-Blm by wtTrxR was considerably slower than reduction by 0.2 mM ascorbate or Cys (Fig. 7A), wtTrxR was actually much faster than ascorbate or cysteine when normalized to each reductant on a molar basis (5.06 μM Fe(II) min^{-1} per μM TrxR; 0.26 μM Fe(II) min^{-1}

per μM ascorbate; 0.057 μM min^{-1} per μM cysteine). However, the rate of Fe(III)-Blm reduction by wtTrxR was 68-fold and 228-fold slower than the rates of Fe(III)$(Dp44mT)_2$ and Fe(III)$(Tp)_2$ reduction (based on μM Fe(II) generated per min per μM TrxR with 50 μM of each Fe(III) complex). The redox centers within TrxR that mediate Fe(III)-Blm reduction are, however, distinctly different from those involved in Fe(III)-thiosemicarbazone reduction. The Sec-deficient truncated variant had ~30% activity compared to wtTrxR in reducing Fe(III)-Blm (Fig. 7C) indicating that the Sec has an important role. In contrast, this truncated variant was faster than wtTrxR in reducing the Fe(III)-thiosemicarbazones (Figs. 4, 6). Surprisingly, the U498C variant was very similar to wtTrxR in its reduction of Fe(III)-Blm (Fig. 7C), which suggests that the C498 can substitute for U498 in this reaction. This is not the case for some other TrxR substrates for which the Sec is essential (e.g. Trx, 9,10-phenanthrenequinone) [28]. Relative to truncated TrxR, further declines in Fe(III)-Blm reduction with the C59S and C64S variants (Fig. 7C) imply some ability of these residues to directly reduce Fe(III)-Blm. The residual rate with the C59S/C64S variant was very slow, indicating very little ability of the flavin to directly reduce Fe(III)-Blm. This was in contrast to the Fe(III)-thiosemicarbazones (Figs. 4, 6) for which the flavin could account for a more substantial fraction of the total reduction rate. While C64 was not needed for Fe(III)-thiosemicarbazone reduction, its contribution to Fe(III)-Blm reduction was on par with that of C59 (Fig. 7C).

Fe(III)-Blm did not significantly elevate O_2 consumption when added to wtTrxR plus NADPH (not shown). The relatively slow rates of Fe(III)-Blm reduction may not have provided for significant elevations in O_2 consumption. In spin trapping experiments, while a small DEPMPO/$HO^{\bullet}$ signal was observed when 0.1 mM Fe(III)-Blm was incubated with NADPH, this signal was not further enhanced by the inclusion of wtTrxR (not shown). Together, the results indicate that TrxR does not significantly reduce Fe(III)-EDTA, but that it reduces Fe(III)-Blm in a largely Sec-dependent manner, which is distinct from the Sec-independent reduction of the Fe(III)-thiosemicarbazones.

3.4 Fe$(Tp)_2$ redox cycling does not inhibit the native enzyme activities of TrxR

While some redox cycling agents, such as Cr(VI) and paraquat, can cause irreversible inactivation of TrxR in cells [57–59], we previously noted that 25 and 50 μM Tp did not inhibit total TrxR activity in A549 cells, even though these treatments caused pronounced oxidation of Trx2 and Prx3 [9]. There was the possibility that Tp could lead to selective inhibition of just one TrxR isoform, but we have now determined that 25 or 50 μM Tp for 24 h does not significantly change the activity of cytosolic TrxR1 or mitochondrial TrxR2 in these cells (Supplemental Fig. S8A). 50 μM Tp similarly does not inhibit GR activity in these cells [9]. We also determined that in vitro incubation of wtTrxR with 25 or 50 μM Fe$(Tp)_2$ in the presence of NADPH for 15 min (in the absence of DEPMPO) does not significantly inhibit TrxR activity (Supplemental Fig. S8B), despite the generation of significant amounts of $HO^{\bullet}$ and carbon radical as shown in the spin trapping experiments. Therefore, the generation of reactive species by Fe$(Tp)_2$ redox cycling does not inhibit the ability of TrxR to continue to reduce Fe(III) complexes, nor does it inhibit other native enzyme activities of TrxR.

3.5 Comparison of the redox activities of GR and TrxR1 with Fe(III)-thiosemicarbazones

While GR lacks the C497/U498 domain of TrxR, GR shares strong homology with the rest of TrxR1, including the flavin and -CVNVGC- dithiol domain (C59/C64 in TrxR) [28, 60] which are important for Fe(III)-thiosemicarbazone reduction by TrxR (Figs. 4, 6). Surprisingly, however, GR reduced Fe(III)$(Tp)_2$ and Fe$(Dp44mT)_2$ at rates that were 46% and 49%, respectively, of wtTrxR1 (Supplemental Fig. S9). Consistent with these slower

rates, GR generated much smaller ESR spin trap signals than wtTrxR or TrxR variants (Supplemental Fig. S9).

4. Discussion

4.1 The enzyme-catalyzed redox cycling of Fe(III)-thiosemicarbazones may contribute to their cytotoxic effects

The results show that TrxR and, to a lesser extent, GR reductively activate Fe(III)-thiosemicarbazones. To our knowledge, this is the first identification of specific enzymes that actively promote redox cycling of these anticancer agents. With TrxR as the reductant, $HO^{\bullet}$ was the predominant trapped species generated in the presence of 2.5–25 μM Fe(III)$(Tp)_2$, and $HO^{\bullet}$ adduct signals were of similar size over this range of Fe$(Tp)_2$ concentrations (Fig. 2). These concentrations are consistent with Tp concentrations that cause Prx3 oxidation in A549 cells [9], with IC_{50} values of Tp for various cancer cell lines [17, 18], and with plasma concentrations of Tp reported in patients [61, 62]. Pharmacokinetic data indicate that Tp or Fe$(Tp)_2$ may accummulate in some cells or tissues over time [61, 63] such that concentrations in some tissues may exceed those measured in the plasma. Along these lines, tridentate ligands such as Tp can form polymeric complexes which are likely to be trapped in cells [64]. Peripheral blood mononuclear cells from Tp-treated patients show an ESR signal that is suggestive of aggregates of Fe$(Tp)_2$ and/or copper-Tp [65], although these signals very likely underestimate total Fe$(Tp)_2$ because only the Fe(III) form yields an ESR signal.

Our data show that wtTrxR reduces Fe(III)$(Tp)_2$ 3.3-fold faster than Fe(III)$(Dp44mT)_2$, which could account for the much greater reactive species generation with Fe$(Tp)_2$. This is consistent with prior implications that Fe$(Tp)_2$ is critical to the cytotoxicity of Tp [7, 16, 19], and with the ability of catalase to protect cancer cells from Tp [5]. This latter observation implies an important role for peroxide or peroxide-derived species in Tp cytotoxicity. The slower rate of reduction of Fe(III)$(Dp44mT)_2$ by TrxR is consistent with the suggestion that non-redox-cycling mechanisms might contribute to the overall cytotoxicity of Dp44mT [16]. It is also possible that other potential cellular reductants are more proficient at reducing Fe(III)$(Dp44mT)_2$ than Fe$(Tp)_2$. For example, although GSH is a relatively slow reductant of these Fe(III)-thiosemicarbazones, GSH (0.1 mM) reduces Fe$(Tp)_2$ more slowly than Fe(III)$(Dp44mT)_2$ (17 and 28 μM min^{-1}, respectively). In contrast, cysteine (0.1 mM) reduces Fe(III)$(Tp)_2$ twice as fast as Fe(III)$(Dp44mT)_2$ (initial rates of 217 and 107 μM min^{-1}, respectively).

Our observation of greater reactive species generation with Fe$(Tp)_2$ is in contrast to experiments by Richardson et al. [16] which showed that the incubation of Fe(II) with either Tp or Dp44mT generated similar levels of $HO^{\bullet}$ (using benzoate hydroxylation as the indicator), indicating a similar ability of the Fe(II) forms of these thiosemicarbazones to mediate Fenton-like reactions. However, these experiments started with Fe(II) and therefore only looked at the Fenton-like reactions, whereas our results were also dependent on the differential rates of reduction of the two Fe(III)-thiosemicarbazones by TrxR.

The reduction of the Fe(III)-thiosemicarbazones by wtTrxR may not, however, be the sole factor limiting redox cycling in these in vitro experiments. When normalized per μmol of wtTrxR, the initial rates of reduction of 25 μM Fe(III)$(Tp)_2$ or Fe(III)$(Dp44mT)_2$ were 20- and 15-fold faster than the O_2 consumption rates. This suggests that re-oxidation of the Fe(II)-thiosemicarbazones could limit the redox cycling rate in our studies. The oxidation of Fe(II)-thiosemicarbazones to their Fe(III) forms is relatively slow under room air [1], so this could contribute to slower O_2 consumption. While peroxide was not added to most of our experiments, the spin trapping studies in which we added additional peroxide (Fig. 1g)

suggest that H_2O_2 generation may be another component that limited redox cycling. Factors which enhance peroxide generation in cells could therefore further enhance Fe(III)-thiosemicarbazone redox cycling and cytotoxicity. Along these lines, it is interesting to note that Tp treatment of cells leads to the oxidation of mitochondrial peroxiredoxin (Prx3) [9], which is the major peroxidase in mitochondria [66]. This implies that Tp treatment can disrupt or overwhelm mitochondrial peroxide defense, and the redox cycling of $Fe(Tp)_2$ could promote these effects.

While TrxR-mediated reactive species signals were considerably smaller with $Fe(Dp44mT)_2$ than with $Fe(Tp)_2$, we also observed $HO^{\bullet}$ generation with $Fe(Dp44mT)_2$. This is in contrast to studies with ascorbate as a reductant in which $HO^{\bullet}$ was not detected with Fe(III)$(Dp44mT)_2$, but $HO^{\bullet}$ was generated with Fe(III)-Dp44mT in which the Fe was not fully liganded [8]. Pre-formed Fe(II) plus two equivalents of Dp44mT were also shown to generate DMPO/$^{\bullet}CH_3$ [8], an indirect indicator of $HO^{\bullet}$ in the presence of the scavenger DMSO.

4.2 Implications for the enhanced susceptibility of cancer cells to thiosemicarbazones

While TrxR/Trx is normally considered to have broad antioxidant functions [24–26], the robust rates of Fe(III)-thiosemicarbazone reduction by TrxR would be expected to promote oxidative stress. Cancer cells tend to be much more susceptible to thiosemicarbazones than normal cells [18, 20], which may be due to a number of factors. Cancer cells typically have markedly elevated levels of transferrin receptor [67–69] which will facilitate enhanced iron uptake and therefore a greater potential to form Fe-thiosemicarbazones [1]. The marked overexpression of TrxR in many cancers [21–23] could further enhance the redox cycling of Fe-thiosemicarbazones relative to normal cells. Cancer cells (e.g. A549 and HeLa) tend to have a large excess of TrxR relative to what is needed to support growth and to support thioredoxin reduction under normal conditions [23, 70]. However, under conditions that enhance oxidant generation, the ability of TrxR to maintain normal thiol redox control can be quickly lost [70]. Thus, the redox cycling of $Fe(Tp)_2$ in cancer cells could be enhanced by their elevated levels of TrxR, and the resulting generation of ROS could promote the oxidation of Trx and Prx as previously reported [9]. While we showed that GR may also contribute to Fe(III)-thiosemicarbazone redox cycling, GR levels in tumors are not consistently elevated compared to normal tissues [71].

4.3 Specificity of the redox centers of TrxR for different Fe(III) complexes

The reduction of several other substrates by TrxR is largely Sec-dependent, including Trx, DTNB, 9,10-phenanthrenequinone, and pyrroloquinoline quinone [28, 72, 73]. We showed that the reduction of Fe(III)-Blm is also largely Sec-dependent (Fig. 7C), whereas the Sec is not required for Fe(III)-thiosemicarbazone reduction. In fact, the Sec-deficient variants are actually faster than wtTrxR at reducing $Fe(Tp)_2$ (Fig. 4C). The absence of the Sec might result in greater electron density on the FAD and C59/C64 motifs which could enhance their ability to reduce Fe(III)$(Tp)_2$. The absence of the Sec also prevents peroxide degradation by TrxR, and the resulting elevated peroxide could enhance the redox cycling of $Fe(Tp)_2$. It is interesting that the U498C variant reduces Fe(III)$(Tp)_2$ even faster than the truncated variant (Fig. 4C). One possibility is that C498 can contribute to Fe(III)$(Tp)_2$ reduction, whereas U498 in wtTrxR is unable (or less able) to reduce Fe(III)$(Tp)_2$. C498 can substitute for U498 in Fe(III)-Blm reduction (Fig. 7C). The results with $Fe(Dp44mT)_2$ were different than the other Fe(III) complexes in that $Fe(Dp44mT)_2$ was reduced at similar rates by wtTrxR and U498C, whereas the truncated variant rate was >-2-fold faster than wtTrxR (Fig. 6).

Because the Sec is not required for Fe(III)-thiosemicarbazone reduction, agents which form adducts with the Sec (e.g. cisplatin, nitrosoureas, dinitrohalobenzenes, and others [25, 28,

32–35, 74]) should not compromise, and may even enhance, the reduction of Fe(III)$(Tp)_2$ by the FAD/C59 of TrxR in cells, such that the pro-oxidant effects of Fe$(Tp)_2$ redox cycling would occur in conjunction with the other cytotoxic effects of these other agents (e.g. cisplatin) [28, 56]. Along these lines, cisplatin can be synergistically cytotoxic with Tp [63, 75]. However, since Fe(III)-Blm reduction is Sec-dependent, we would predict that Sec-targeting inhibitors would decrease the ability of TrxR to reduce Fe(III)-Blm.

The results further indicate that the C59 and FAD of TrxR can largely account for its reduction of Fe(III)-thiosemicarbazones, whereas C64 is not required (Figs. 4, 6). During normal catalysis, the EH_4 state of wtTrxR has two electrons on the C497/U498 domain, one on C59, and the fourth on a charge-transfer complex between the FAD and C64 [28, 30]. This reduced C59 thiol might facilitate the direct reduction of substrates such as Fe(III)-thiosemicarbazones. In the C59S/C64S variant, the flavin is likely directly reducing the Fe(III)-thiosemicarbazones, although at a considerably slower rate relative to wtTrxR. The C59/C64 dithiol is not required for FAD reduction by NADPH, so the flavin in NADPH-reduced C59S/C64S is likely $FADH_2$. Unlike some other reduced flavoproteins, however, the reduced flavin of TrxR does not directly generate $O_2^{\bullet -}$ at an appreciable rate [41]. Since the C59 and C64 residues are important for the inherent NADPH oxidase activity of TrxR, the C59S and C64S variants cannot directly generate $O_2^{\bullet -}$ [41]. This eliminates direct $O_2^{\bullet -}$ generation by the C59S and C59S/C64S variants as a possible explanation for their reduction of Fe(III)-thiosemicarbazones. Consistent with this, SOD did not alter the levels of $HO^{\bullet}$ or $C^{\bullet}$ adducts generated by C59S plus Fe(III)$(Tp)_2$ (Fig. 5E).

Despite the similarity in the flavin and -CVNVGC- (C59/C64 in TrxR) domains of TrxR and GR, TrxR was considerably faster than GR at reducing both Fe(III)$(Tp)_2$ and Fe(III)$(Dp44mT)_2$. This might be due to the different predicted electrostatic potentials of their N-terminal-CVNVGC- domains (positively charged in GR but negatively charged in TrxR [76]). Along these lines, GR favors the binding of negatively charged substrates such as GSSG, whereas TrxR cannot reduce GSSG [76]. Conversely, this charge differential could favor the binding of Fe(III)$(Tp)_2$ (which has a net +1 charge [1, 64]) to TrxR compared to GR. This charge differential may not be the sole explanation, however. For example, juglone is also more efficiently reduced by the N-terminal dithiol of TrxR than by GR [72], but it is not clear if the N-terminal electrostatic charge differences influence juglone reduction. Other factors that could conceivably contribute to different reduction rates of Fe(III) complexes by these enzymes include accessibility of the enzyme redox centers, accessibility of the Fe(III) centers in the different complexes, and non-equilibrium conditions. It is unlikely, however, that differences in redox potentials of TrxR and GR account for the different rates. TrxR mainly cycles between the four-electron reduced (EH_4) and two-electron reduced (EH_2) states, and the redox potential of this couple is −294 mV at pH 7.0 (calculated according to the Haldane relationship with NADPH/$NADP^+$) [73]. The redox potential of catalytically active GR is −206 mV (at pH 6.9 for the E_{ox}/EH_2 redox couple) [77]. Thus, while TrxR is suggested to have a lower redox potential than GR, both enzymes should have sufficient redox potential to reduce the Fe(III) complexes used here. Similarly, redox potentials of the Fe(III) complexes do not likely account for different rates by TrxR or GR, or for different rates of reduction of the different Fe(III) species. Fe(III)$(Tp)_2$ has the least positive reduction potential (+40 mV) [78] of those tested here, but yet it is reduced considerably faster than Fe(III)$(Dp44mT)_2$ (+113 to +166 mV) [16, 78]. TrxR reduces Fe(III)-Blm (+129 mV) [79] at a much slower rate, and does not significantly reduce Fe(III)-EDTA (+120 mV) [80] even though their redox potentials are in the same range. EDTA is not large enough to completely protect the liganded Fe(III) [64], and Fe(III)-EDTA can be reduced and redox-cycled by other chemical and enzymatic reductants [81], including NADPH:P450 reductase (a flavoprotein with FAD and FMN centers) and cytochrome b_5 [82, 83].

Together, our results demonstrate that there is a high degree of specificity of the individual redox centers in TrxR1 for different Fe(III) complexes, and there are considerable differences in the rates at which different Fe(III) species are reduced by TrxR. While our studies used TrxR1 (the cytosolic isoform), the mitochondrial isoform (TrxR2) shares the same redox centers, so it is plausible that TrxR2 can similarly reduce Fe(III)-thiosemicarbazones and Fe(III)-Blm. TrxR1 and TrxR2 share similar kinetics with some substrates (e.g. Trx2), but kinetic differences have been observed with others (e.g. Trx1 or DTNB) [42].

4.4 Conclusions

In summary, this is the first identification of specific enzymes promoting the redox cycling of Fe(III) thiosemicarbazones. TrxR has pronounced ability to reduce Fe(III)-thiosemicarbazones, especially $Fe(Tp)_2$. This reduction promotes redox cycling and the generation of $HO^{\bullet}$ at even low μM levels of $Fe(Tp)_2$, and $HO^{\bullet}$ generation by this system is largely peroxide-dependent. The reduction of Fe(III)-thiosemicarbazones by TrxR1 does not require its Sec, but the C59 and flavin are important for this activity. GR has these two latter motifs and it can reduce Fe(III)-thiosemicarbazones, although at slower rates than TrxR. In contrast, the reduction of Fe(III)-Blm by TrxR is largely Sec-dependent, and the rates are considerably slower than for the Fe(III)-thiosemicarbazones. TrxR cannot reduce or redox cycle Fe(III)-EDTA at significant rates. These results suggest that the reduction of different Fe(III) complexes by TrxR is highly specific with regard to individual redox centers and that TrxR may play a role in enhancing the efficacy of Fe(III)-based antitumor agents for which Fe(III) reduction is critical to their cytotoxic activity. Enzymes with analogous redox centers, such as GR, may also have a role in promoting their cytotoxic effects, but GR was less efficient than TrxR1. Because TrxR1 is often overexpressed in tumor cells, we believe that it should hereby be considered to have a potentially key role in Fe(III)-based anticancer chemotherapy.

Supplementary Material

Refer to Web version on PubMed Central for supplementary material.

Acknowledgments

This research was supported by a grant awarded to C. Myers from the Cancer Center of the Medical College of Wisconsin (State of Wisconsin Tax Check-Off Program), and by grants awarded to E. Arnér by the Swedish Research Council (Medicine), the Swedish Cancer Society, the Knut and Alice Wallenberg Foundation, and the Karolinska Institutet. Additional support was provided by the Dept. of Pharmacology and Toxicology and the Dept. of Biophysics of the Medical College of Wisconsin. The ESR facilities were supported by National Biomedical ESR Center Grant EB001980 from the NIH (awarded to the Dept. Biophysics, Medical College of Wisconsin). Triapine was provided by Vion Pharmaceuticals (New Haven, CT).

Abbreviations

Blm	bleomycin
BPS	bathophenanthroline disulfonate
Cys	cysteine
DEPMPO	5-diethoxyphos-phoryl-5-methyl-1-pyrroline-*N*-oxide
DMPO	5,5,-dimethyl-1-pyrroline *N*-oxide
DMSO	dimethylsulfoxide
Dp44mT	2,2′-Dipyridyl-N,N-dimethylsemicarbazone

DTNB	5,5′-dithiobis(2-nitrobenzoic) acid
ESR	electron spin resonance
GR	glutathione reductase
GSH	reduced glutathione
$HO^{\bullet}$	hydroxyl radical
$^{\bullet}CH_3$	methyl radical
$O_2^{\bullet -}$	superoxide
PBN	-phenyl-*N*-*tert*-butylnitrone
ROS	reactive oxygen species
RR	ribonucleotide reductase
Sec	selenocysteine
SOD	superoxide dismutase
Tp	triapine
Trx2	thioredoxin-2
TrxR	thioredoxin reductase
wtTrxR	wild-type thioredoxin reductase

References

1. Yu Y, Kalinowski DS, Kovacevic Z, Siafakas AR, Jansson PJ, Stefani C, Lovejoy DB, Sharpe PC, Bernhardt PV, Richardson DR. Thiosemicarbazones from the old to new: iron chelators that are more than just ribonucleotide reductase inhibitors. J Med Chem. 2009; 52:5271–5294. [PubMed: 19601577]
2. Petering, DH.; Antholine, WE.; Saryan, LA. Metal complexes as antitumor agents. In: Ottenbrite, RM.; Butler, GB., editors. Anticancer and Interferon Agents. New York: Marcell Dekker; 1984. p. 203-246.
3. Chitambar CR, Antholine WE. Iron-targeting antitumor activity of gallium compounds and novel insights into triapine((R))-metal complexes. Antioxid Redox Signal. 2013; 18:956–972. [PubMed: 22900955]
4. Kalinowski DS, Richardson DR. Future of toxicology--iron chelators and differing modes of action and toxicity: the changing face of iron chelation therapy. Chem Res Toxicol. 2007; 20:715–720. [PubMed: 17402750]
5. Shao J, Zhou B, Di Bilio AJ, Zhu L, Wang T, Qi C, Shih J, Yen Y. A Ferrous-Triapine complex mediates formation of reactive oxygen species that inactivate human ribonucleotide reductase. Mol Cancer Ther. 2006; 5:586–592. [PubMed: 16546972]
6. Popovic-Bijelic A, Kowol CR, Lind ME, Luo J, Himo F, Enyedy ÉA, Arion VB, Gräslund A. Ribonucleotide reductase inhibition by metal complexes of Triapine (3-aminopyridine-2-carboxaldehyde thiosemicarbazone): a combined experimental and theoretical study. J Inorg Biochem. 2011; 105:1422–1431. [PubMed: 21955844]
7. Finch RA, Liu MC, Cory AH, Cory JG, Sartorelli AC. Triapine (3-aminopyridine-2-carboxaldehyde thiosemicarbazone; 3-AP): an inhibitor of ribonucleotide reductase with antineoplastic activity. Adv Enzyme Regul. 1999; 39:3–12. [PubMed: 10470363]
8. Jansson PJ, Hawkins CL, Lovejoy DB, Richardson DR. The iron complex of Dp44mT is redox-active and induces hydroxyl radical formation: an EPR study. J Inorg Biochem. 2010; 104:1224–1228. [PubMed: 20719391]

9. Myers JM, Antholine WE, Myers CR. The iron-chelating drug triapine causes pronounced mitochondrial thiol redox stress. Toxicol Lett. 2011; 201:130–136. [PubMed: 21195754]
10. Peskin AV, Low FM, Paton LN, Maghzal GJ, Hampton MB, Winterbourn CC. The high reactivity of peroxiredoxin 2 with H_2O_2 is not reflected in its reaction with other oxidants and thiol reagents. J Biol Chem. 2007; 282:11885–11892. [PubMed: 17329258]
11. Stipanuk MH, Londono M, Lee JI, Hu M, Yu AF. Enzymes and metabolites of cysteine metabolism in nonhepatic tissues of rats show little response to changes in dietary protein or sulfur amino acid levels. J Nutr. 2002; 132:3369–3378. [PubMed: 12421853]
12. Lee JI, Londono M, Hirschberger LL, Stipanuk MH. Regulation of cysteine dioxygenase and gamma-glutamylcysteine synthetase is associated with hepatic cysteine level. J Nutr Biochem. 2004; 15:112–122. [PubMed: 14972351]
13. Schafer FQ, Buettner GR. Redox environment of the cell as viewed through the redox state of the glutathione disulfide/glutathione couple. Free Radic Biol Med. 2001; 30:1191–1212. [PubMed: 11368918]
14. Yuan J, Lovejoy DB, Richardson DR. Novel di-2-pyridyl-derived iron chelators with marked and selective antitumor activity: in vitro and in vivo assessment. Blood. 2004; 104:1450–1458. [PubMed: 15150082]
15. Sigmond J, Kamphuis JA, Laan AC, Hoebe EK, Bergman AM, Peters GJ. The synergistic interaction of gemcitabine and cytosine arabinoside with the ribonucleotide reductase inhibitor triapine is schedule dependent. Biochem Pharmacol. 2007; 73:1548–1557. [PubMed: 17324380]
16. Richardson DR, Sharpe PC, Lovejoy DB, Senaratne D, Kalinowski DS, Islam M, Bernhardt PV. Dipyridyl thiosemicarbazone chelators with potent and selective antitumor activity form iron complexes with redox activity. J Med Chem. 2006; 49:6510–6521. [PubMed: 17064069]
17. Alvero AB, Chen W, Sartorelli AC, Schwartz P, Rutherford T, Mor G. Triapine (3-aminopyridine-2-carboxaldehyde thiosemicarbazone) induces apoptosis in ovarian cancer cells. J Soc Gynecol Investig. 2006; 13:145–152.
18. Whitnall M, Howard J, Ponka P, Richardson DR. A class of iron chelators with a wide spectrum of potent antitumor activity that overcomes resistance to chemotherapeutics. Proc Natl Acad Sci U S A. 2006; 103:14901–14906. [PubMed: 17003122]
19. Chaston TB, Lovejoy DB, Watts RN, Richardson DR. Examination of the antiproliferative activity of iron chelators: multiple cellular targets and the different mechanism of action of triapine compared with desferrioxamine and the potent pyridoxal isonicotinoyl hydrazone analogue 311. Clin Cancer Res. 2003; 9:402–414. [PubMed: 12538494]
20. Kalinowski DS, Richardson DR. The evolution of iron chelators for the treatment of iron overload disease and cancer. Pharmacol Rev. 2005; 57:547–583. [PubMed: 16382108]
21. Soini Y, Kahlos K, Napankangas U, Kaarteenaho-Wiik R, Saily M, Koistinen P, Paaakko P, Holmgren A, Kinnula VL. Widespread expression of thioredoxin and thioredoxin reductase in non-small cell lung carcinoma. Clin Cancer Res. 2001; 7:1750–1757. [PubMed: 11410516]
22. Lincoln DT, Ali Emadi EM, Tonissen KF, Clarke FM. The thioredoxin-thioredoxin reductase system: over-expression in human cancer. Anticancer Res. 2003; 23:2425–2433. [PubMed: 12894524]
23. Eriksson SE, Prast-Nielsen S, Flaberg E, Szekely L, Arnér ES. High levels of thioredoxin reductase 1 modulate drug-specific cytotoxic efficacy. Free Radic Biol Med. 2009; 47:1661–1671. [PubMed: 19766715]
24. Kumar S, Bjornstedt M, Holmgren A. Selenite is a substrate for calf thymus thioredoxin reductase and thioredoxin and elicits a large non-stoichiometric oxidation of NADPH in the presence of oxygen. Eur J Biochem. 1992; 207:435–439. [PubMed: 1321713]
25. Nordberg J, Arnér ES. Reactive oxygen species, antioxidants, and the mammalian thioredoxin system. Free Radic Biol Med. 2001; 31:1287–1312. [PubMed: 11728801]
26. Bjornstedt M, Hamberg M, Kumar S, Xue J, Holmgren A. Human thioredoxin reductase directly reduces lipid hydroperoxides by NADPH and selenocystine strongly stimulates the reaction via catalytically generated selenols. J Biol Chem. 1995; 270:11761–11764. [PubMed: 7744824]
27. Cheng Q, Sandalova T, Lindqvist Y, Arnér ES. Crystal structure and catalysis of the selenoprotein thioredoxin reductase 1. J Biol Chem. 2009; 284:3998–4008. [PubMed: 19054767]

28. Arnér ES. Focus on mammalian thioredoxin reductases--important selenoproteins with versatile functions. Biochim Biophys Acta. 2009; 1790:495–526. [PubMed: 19364476]
29. Powis G, Montfort WR. Properties and biological activities of thioredoxins. Annu Rev Biophys Biomol Struct. 2001; 30:421–455. [PubMed: 11441809]
30. Zhong L, Arnér ES, Holmgren A. Structure and mechanism of mammalian thioredoxin reductase: the active site is a redox-active selenolthiol/selenenylsulfide formed from the conserved cysteine-selenocysteine sequence. Proc Natl Acad Sci U S A. 2000; 97:5854–5859. [PubMed: 10801974]
31. Zhong L, Holmgren A. Essential role of selenium in the catalytic activities of mammalian thioredoxin reductase revealed by characterization of recombinant enzymes with selenocysteine mutations. J Biol Chem. 2000; 275:18121–18128. [PubMed: 10849437]
32. Nordberg J, Zhong L, Holmgren A, Arnér ES. Mammalian thioredoxin reductase is irreversibly inhibited by dinitrohalobenzenes by alkylation of both the redox active selenocysteine and its neighboring cysteine residue. J Biol Chem. 1998; 273:10835–10842. [PubMed: 9556556]
33. Witte AB, Anestål K, Jerremalm E, Ehrsson H, Arnér ES. Inhibition of thioredoxin reductase but not of glutathione reductase by the major classes of alkylating and platinum-containing anticancer compounds. Free Radic Biol Med. 2005; 39:696–703. [PubMed: 16085187]
34. Gromer S, Urig S, Becker K. The thioredoxin system--from science to clinic. Med Res Rev. 2004; 24:40–89. [PubMed: 14595672]
35. Urig S, Becker K. On the potential of thioredoxin reductase inhibitors for cancer therapy. Semin Cancer Biol. 2006; 16:452–465. [PubMed: 17056271]
36. Lothrop AP, Ruggles EL, Hondal RJ. No selenium required: reactions catalyzed by mammalian thioredoxin reductase that are independent of a selenocysteine residue. Biochemistry. 2009; 48:6213–6223. [PubMed: 19366212]
37. Arnér ES. Recombinant expression of mammalian selenocysteine-containing thioredoxin reductase and other selenoproteins in Escherichia coli. Meth Enzymol. 2002; 347:226–235. [PubMed: 11898411]
38. Cheng Q, Stone-Elander S, Arnér ES. Tagging recombinant proteins with a Sel-tag for purification, labeling with electrophilic compounds or radiolabeling with 11C. Nat Protoc. 2006; 1: 604–613. [PubMed: 17406287]
39. Johansson L, Chen C, Thorell JO, Fredriksson A, Stone-Elander S, Gafvelin G, Arnér ES. Exploiting the 21st amino acid-purifying and labeling proteins by selenolate targeting. Nat Methods. 2004; 1:61–66. [PubMed: 15782154]
40. Rengby O, Johansson L, Carlson LA, Serini E, Vlamis-Gardikas A, Karsnas P, Arnér ES. Assessment of production conditions for efficient use of *Escherichia coli* in high-yield heterologous recombinant selenoprotein synthesis. Appl Environ Microbiol. 2004; 70:5159–5167. [PubMed: 15345395]
41. Cheng Q, Antholine WE, Myers JM, Kalyanaraman B, Arnér ES, Myers CR. The selenium-independent inherent pro-oxidant NADPH oxidase activity of mammalian thioredoxin reductase and its selenium-dependent direct peroxidase activities. J Biol Chem. 2010; 285:21708–21723. [PubMed: 20457604]
42. Rackham O, Shearwood AM, Thyer R, McNamara E, Davies SM, Callus BA, Miranda-Vizuete A, Berners-Price SJ, Cheng Q, Arnér ES, Filipovska A. Substrate and inhibitor specificities differ between human cytosolic and mitochondrial thioredoxin reductases: Implications for development of specific inhibitors. Free Radic Biol Med. 2011; 50:689–699. [PubMed: 21172426]
43. Wang Y, Qiao M, Mieyal JJ, Asmis LM, Asmis R. Molecular mechanism of glutathione-mediated protection from oxidized low-density lipoprotein-induced cell injury in human macrophages: role of glutathione reductase and glutaredoxin. Free Radic Biol Med. 2006; 41:775–785. [PubMed: 16895798]
44. Myers CR, Myers JM. Iron stimulates the rate of reduction of hexavalent chromium by human microsomes. Carcinogenesis. 1998; 19:1029–1038. [PubMed: 9667741]
45. Borthiry GR, Antholine WE, Kalyanaraman B, Myers JM, Myers CR. Reduction of hexavalent chromium by human cytochrome b_5: Generation of hydroxyl radical and superoxide. Free Radic Biol Med. 2007; 42:738–755. [PubMed: 17320757]

46. Frejaville C, Karoui H, Tuccio B, Le Moigne F, Culcasi M, Pietri S, Lauricella R, Tordo P. 5-(Diethoxyphosphoryl)-5-methyl-1-pyrroline *N*-oxide: a new efficient phosphorylated nitrone for the in vitro and in vivo spin trapping of oxygen-centered radicals. J Med Chem. 1995; 38:258–265. [PubMed: 7830268]
47. Tordo, P. Spin-trapping: recent developments and applications. In: Gilbert, BC.; Atherton, NM.; Davies, MJ., editors. Electron Paramagnetic Resonance Specialist Periodical Reports. Cambridge: The Royal Society of Chemistry; 1998. p. 116-144.
48. Duling DR. Simulation of multiple isotropic spin-trap EPR spectra. J Magn Reson B. 1994; 104:105–110. [PubMed: 8049862]
49. Li W, Antholine WE, Petering DH. Kinetics of reaction of DNA-bound Fe(III)bleomycin with ascorbate: interplay of specific and non-specific binding. J Inorg Biochem. 2002; 90:8–17. [PubMed: 12009250]
50. Antholine WE, Petering DH. On the reaction of iron bleomycin with thiols and oxygen. Biochem Biophys Res Commun. 1979; 90:384–389. [PubMed: 91373]
51. Vásquez-Vivar J, Hogg N, Martásek P, Karoui H, Tordo P, Pritchard KAJ, Kalyanaraman B. Effect of redox-active drugs on superoxide generation from nitric oxide synthases: biological and toxicological implications. Free Radic Res. 1999; 31:607–617. [PubMed: 10630684]
52. Singh RJ, Karoui H, Gunther MR, Beckman JS, Mason RP, Kalyanaraman B. Reexamination of the mechanism of hydroxyl radical adducts formed from the reaction between familial amyotrophic lateral sclerosis-associated Cu,Zn superoxide dismutase mutants and H_2O_2. Proc Natl Acad Sci USA. 1998; 95:6675–6680. [PubMed: 9618471]
53. Ueda J, Takeshita K, Matsumoto S, Yazaki K, Kawaguchi M, Ozawa T. Singlet oxygen-mediated hydroxyl radical production in the presence of phenols: whether DMPO-•OH formation really indicates production of •OH? Photochem Photobiol. 2003; 77:165–170. [PubMed: 12785055]
54. Mitroka S, Zimmeck S, Troya D, Tanko JM. How solvent modulates hydroxyl radical reactivity in hydrogen atom abstractions. J Am Chem Soc. 2010; 132:2907–2913. [PubMed: 20146469]
55. Karoui H, Hogg N, Fréjaville C, Tordo P, Kalyanaraman B. Characterization of sulfur-centered radical intermediates formed during the oxidation of thiols and sulfite by peroxynitrite. J Biol Chem. 1996; 271:6000–6009. [PubMed: 8626383]
56. Anestål K, Prast-Nielsen S, Cénas N, Arnér ES. Cell death by SecTRAPs: thioredoxin reductase as a prooxidant killer of cells. PLoS ONE. 2008; 3:e1846. [PubMed: 18382651]
57. Myers JM, Myers CR. The effects of hexavalent chromium on thioredoxin reductase and peroxiredoxins in human bronchial epithelial cells. Free Radic Biol Med. 2009; 47:1477–1485. [PubMed: 19703554]
58. Myers CR. The effects of chromium(VI) on the thioredoxin system: Implications for redox regulation. Free Radic Biol Med. 2012; 52:2091–2107. [PubMed: 22542445]
59. Takizawa M, Komori K, Tampo Y, Yonaha M. Paraquat-induced oxidative stress and dysfunction of cellular redox systems including antioxidative defense enzymes glutathione peroxidase and thioredoxin reductase. Toxicol In Vitro. 2007; 21:355–363. [PubMed: 17055214]
60. Sandalova T, Zhong L, Lindqvist Y, Holmgren A, Schneider G. Three-dimensional structure of a mammalian thioredoxin reductase: implications for mechanism and evolution of a selenocysteine-dependent enzyme. Proc Natl Acad Sci USA. 2001; 98:9533–9538. [PubMed: 11481439]
61. Wadler S, Makower D, Clairmont C, Lambert P, Fehn K, Sznol M. Phase I and pharmacokinetic study of the ribonucleotide reductase inhibitor, 3-aminopyridine-2-carboxaldehyde thiosemicarbazone, administered by 96-hour intravenous continuous infusion. J Clin Oncol. 2004; 22:1553–1563. [PubMed: 15117978]
62. Kolesar J, Brundage RC, Pomplun M, Alberti D, Holen K, Traynor A, Ivy P, Wilding G. Population pharmacokinetics of 3-aminopyridine-2-carboxaldehyde thiosemicarbazone (Triapine®) in cancer patients. Cancer Chemother Pharmacol. 10.1017/s00280-010-1331-z:2010
63. Kunos CA, Waggoner S, von Gruenigen V, Eldermire E, Pink J, Dowlati A, Kinsella TJ. Phase I trial of pelvic radiation, weekly cisplatin, and 3-aminopyridine-2-carboxaldehyde thiosemicarbazone (3-AP, NSC #663249) for locally advanced cervical cancer. Clin Cancer Res. 2010; 16:1298–1306. [PubMed: 20145183]

64. Liu ZD, Hider RC. Design of iron chelators with therpaeutic application. Coord Chem Rev. 2002; 232:151–171.
65. Kolesar JM, Schelman WR, Geiger PG, Holen KD, Traynor AM, Alberti DB, Thomas JP, Chitambar CR, Wilding G, Antholine WE. Electron paramagnetic resonance study of peripheral blood mononuclear cells from patients with refractory solid tumors treated with Triapine. J Inorg Biochem. 2008; 102:693–698. [PubMed: 18061679]
66. Cox AG, Winterbourn CC, Hampton MB. Mitochondrial peroxiredoxin involvement in antioxidant defence and redox signalling. Biochem, J. 2010; 425:313–325.
67. Walker RA, Day SJ. Transferrin receptor expression in non-malignant and malignant human breast tissue. J Pathol. 1986; 148:217–224. [PubMed: 3009766]
68. Hogemann-Savellano D, Bos E, Blondet C, Sato F, Abe T, Josephson L, Weissleder R, Gaudet J, Sgroi D, Peters PJ, Basilion JP. The transferrin receptor: a potential molecular imaging marker for human cancer. Neoplasia. 2003; 5:495–506. [PubMed: 14965443]
69. Daniels TR, Delgado T, Rodriguez JA, Helguera G, Penichet ML. The transferrin receptor part I: Biology and targeting with cytotoxic antibodies for the treatment of cancer. Clin Immunol. 2006; 121:144–158. [PubMed: 16904380]
70. Watson WH, Heilman JM, Hughes LL, Spielberger JC. Thioredoxin reductase-1 knock down does not result in thioredoxin-1 oxidation. Biochem Biophys Res Commun. 2008; 368:832–836. [PubMed: 18267104]
71. Singh SV, Brunnert SR, Roberts B, Krishan A. Differential expression of glutathione S-transferase, glutathione peroxidase and glutathione reductase in normal and malignant human breast tissues. Cancer Lett. 1990; 51:43–48. [PubMed: 2337897]
72. Xu J, Arnér ES. Pyrroloquinoline quinone modulates the kinetic parameters of the mammalian selenoprotein thioredoxin reductase 1 and is an inhibitor of glutathione reductase. Biochem Pharmacol. 2012; 83:815–820. [PubMed: 22226931]
73. Cénas N, Nivinskas H, Anusevicius Z, Sarlauskas J, Lederer F, Arnér ES. Interactions of quinones with thioredoxin reductase: a challenge to the antioxidant role of the mammalian selenoprotein. J Biol Chem. 2004; 279:2583–2592. [PubMed: 14604985]
74. Arnér ES, Nakamura H, Sasada T, Yodoi J, Holmgren A, Spyrou G. Analysis of the inhibition of mammalian thioredoxin, thioredoxin reductase, and glutaredoxin by cis-diamminedichloroplatinum (II) and its major metabolite, the glutathione-platinum complex. Free Radic Biol Med. 2001; 31:1170–1178. [PubMed: 11705695]
75. Finch RA, Liu M, Grill SP, Rose WC, Loomis R, Vasquez KM, Cheng Y, Sartorelli AC. Triapine (3-aminopyridine-2-carboxaldehyde- thiosemicarbazone): A potent inhibitor of ribonucleotide reductase activity with broad spectrum antitumor activity. Biochem Pharmacol. 2000; 59:983–991. [PubMed: 10692563]
76. Urig S, Lieske J, Fritz-Wolf K, Irmler A, Becker K. Truncated mutants of human thioredoxin reductase 1 do not exhibit glutathione reductase activity. FEBS Lett. 2006; 580:3595–3600. [PubMed: 16750198]
77. Böhme CC, Arscott LD, Becker K, Schirmer RH, Williams CH Jr. Kinetic characterization of glutathione reductase from the malarial parasite Plasmodium falciparum. Comparison with the human enzyme. J Biol Chem. 2000; 275:37317–37323. [PubMed: 10969088]
78. Quach P, Gutierrez E, Basha MT, Kalinowski DS, Sharpe PC, Lovejoy DB, Bernhardt PV, Jansson PJ, Richardson DR. Methemoglobin formation by Triapine, Di-2-pyridylketone-4,4-dimethyl-3-thiosemicarbazone (Dp44mT), and other anticancer thiosemicarbazones: identification of novel thiosemicarbazones and therapeutics that prevent this effect. Mol Pharmacol. 2012; 82:105–114. [PubMed: 22508546]
79. Melnyk DL, Horwitz SB, Peisach J. Redox potential of iron-bleomycin. Biochemistry. 1981; 20:5327–5331. [PubMed: 6170321]
80. Buettner GR. The pecking order of free radicals and antioxidants: lipid peroxidation, alpha-tocopherol, and ascorbate. Arch Biochem Biophys. 1993; 300:535–543. [PubMed: 8434935]
81. Hasinoff BB. NADPH-cytochrome-P450 reductase promotes hydroxyl radical production by the iron complex of ADR-925, the hydrolysis product of ICRF-187 (dexrazoxane). Free Radic Res. 1995; 22:319–325. [PubMed: 7633562]

82. Morehouse LA, Thomas CE, Aust SD. Superoxide generation by NADPH-cytochrome P-450 reductase: the effect of iron chelators and the role of superoxide in microsomal lipid peroxidation. Arch Biochem Biophys. 1984; 232:366–377. [PubMed: 6331320]

83. Bilimoria MH, Kamin H. The effect of high salt concentrations upon cytochrome *c*, cytochrome *b*5, and iron-EDTA reductase activities of liver microsomal NADPH-cytochrome *c* reductase. Ann N Y Acad Sci. 1973; 212:428–448. [PubMed: 4217577]

Highlights

- Redox cycling of iron-thiosemicarbazones can contribute to their anti-cancer activity.
- Thioredoxin reductase (TrxR) efficiently catalyzes this redox cycling.
- C59 and the flavin of TrxR are involved, whereas the selenocysteine is not required.
- In contrast, iron-bleomycin reduction by TrxR is largely selenocysteine-dependent.
- TrxR overexpression in many tumors could promote thiosemibarbazone efficacy.

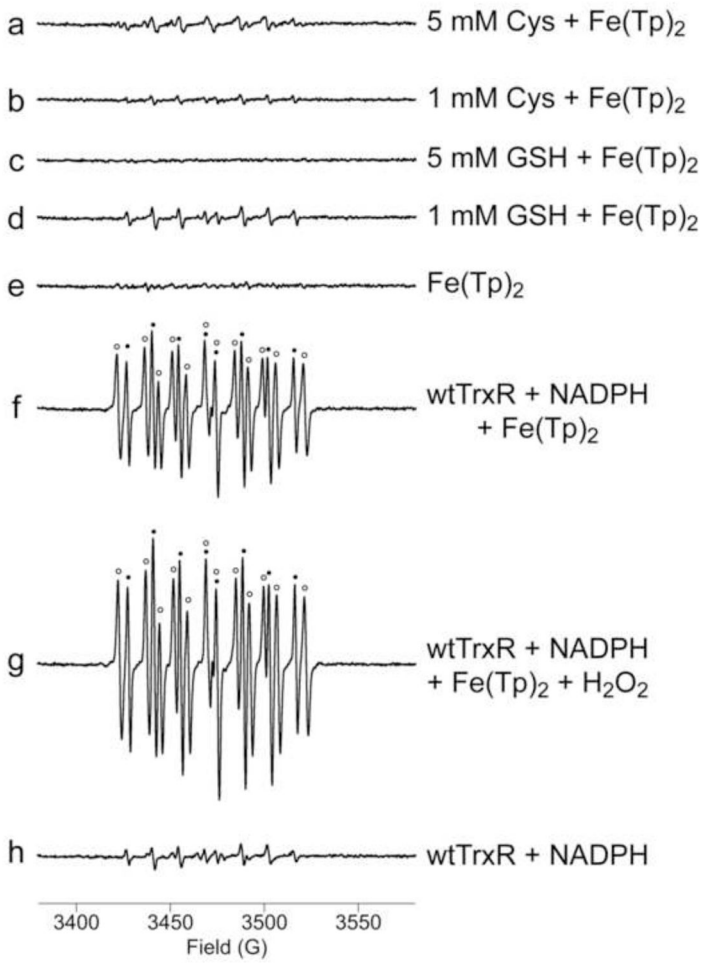

Fig. 1.

Representative ESR spin trapping spectra of radicals formed during the reduction of Fe(III)$(Tp)_2$ by Cys, GSH, or wild-type TrxR. Samples were incubated at 37°C under room air for 15 min. All samples included DEPMPO (14 mM) and Fe(III)$(Tp)_2$ (50 μM) (except for h), as well as: (a) 5 mM Cys; (b) 1 mM Cys; (c) 5 mM GSH; (d) 1 mM GSH; (e) no reductant; (f) 0.3 μM wtTrxR and 0.4 mM NADPH; (g) wtTrxR, NADPH, and 50 μM H_2O_2; (h) wtTrxR and NADPH but without Fe(III)$(Tp)_2$. In f and g, the components of the signal corresponding to DEPMPO/$HO^{\bullet}$ (a^P = 47.2 G, a^H = 13.8 G, a^N = 13.8 G) [55] are indicated by black dots, whereas those corresponding to a carbon radical adduct of DEPMPO (a^P = 47.7 G, a^H = 21.8 G, a^N = 14.7 G) are indicated with open circles. ESR instrument settings were as follows: 1 G modulation amplitude, 19.92 mW microwave power, 6.32 x 10^4 receiver gain, 40.96 ms time constant, 9.76 GHz microwave frequency, sweep width = 200 G, field set = 3480 G, modulation frequency = 100 kHz, scan time = 42 s; number of scans, 9.

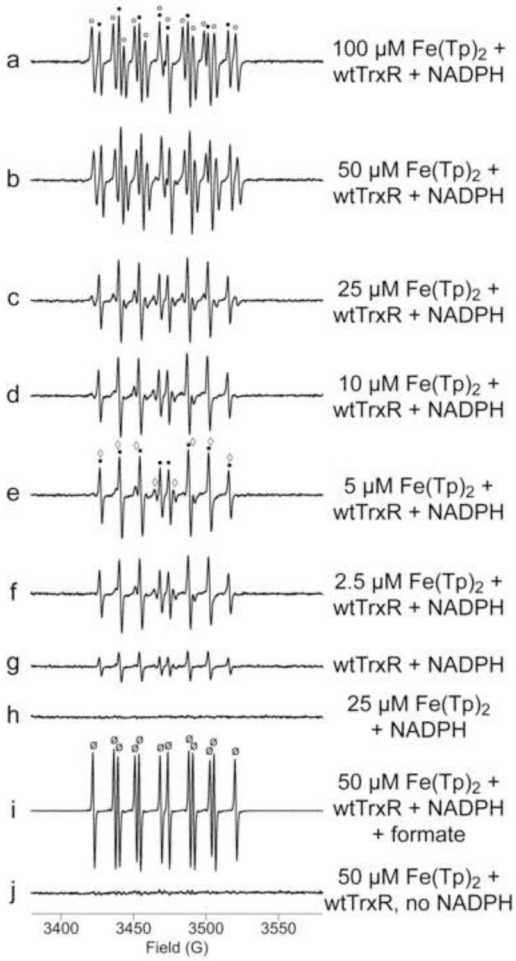

Fig. 2.

Representative ESR spectra of different concentrations of Fe(III)$(Tp)_2$ incubated with wtTrxR. Samples were incubated for 15 min at 37°C under room air, and contained 14 mM DEPMPO, 0.3 μM wtTrxR, 0.4 mM NADPH (a–i), and varied concentrations of Fe(III)$(Tp)_2$ as indicated. Controls included: (g) TrxR and NADPH without Fe(III)$(Tp)_2$, (h) NADPH and Fe$(Tp)_2$ without TrxR, and (j) TrxR and Fe(III)$(Tp)_2$ without NADPH. Sample (i) is the same as b except that 250 mM ammonium formate was included. In (i), the signal intensity was 10-fold greater than shown. This enhanced signal intensity is consistent with increased stability of the DEPMPO/$CO_2^{\bullet -}$ adduct relative to that of other DEPMPO adducts such as DEPMPO/$HO^{\bullet}$. The components of the signal corresponding to DEPMPO/$HO^{\bullet}$ are indicated by black dots (a, e), those corresponding to the carbon radical adduct of DEPMPO are indicated with open circles (a), those for $O_2^{\bullet -}$ adducts are marked with open diamonds (e), and those for the $CO_2^{\bullet -}$ adduct are marked with ø (i). See Fig. 1 for the ESR instrument settings.

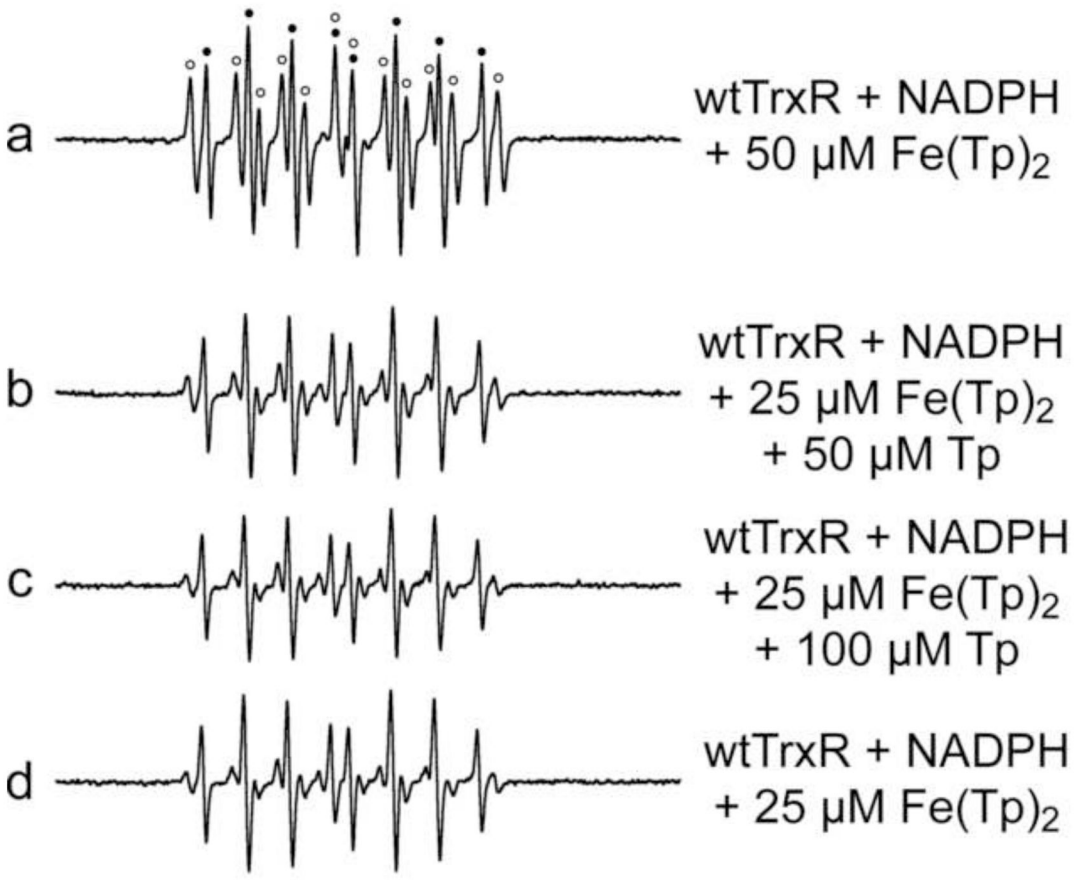

Fig. 3.

Representative ESR spectra comparing the potential effects of excess free Tp when incubated with wtTrxR and Fe(III)$(Tp)_2$. Samples were incubated for 15 min at 37°C under room air, and contained 14 mM DEPMPO, 0.3 μM wtTrxR, 0.4 mM NADPH, and varied concentrations of Fe(III)$(Tp)_2$ and Tp as indicated. For spectrum a, components of the signal corresponding to DEPMPO/$HO^{\bullet}$ are indicated by black dots, whereas those corresponding to the carbon radical adduct of DEPMPO are indicated with open circles. See Fig. 1 for the ESR instrument settings.

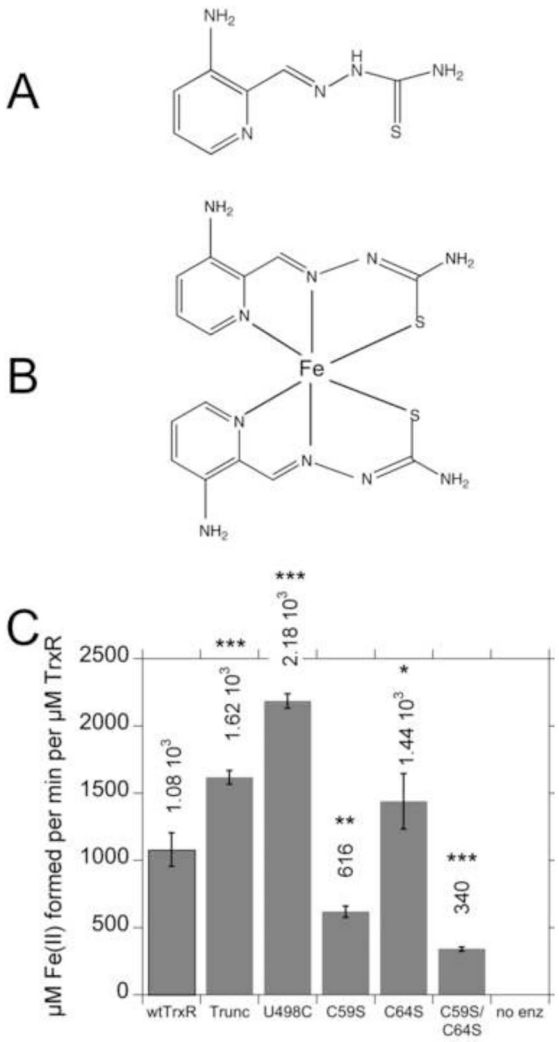

Fig. 4.

Chemical structures of Tp (A) and $Fe(Tp)_2$ (B), and (C) rates of reduction of $Fe(III)(Tp)_2$ by wtTrxR and its site-directed variants. In B, the $Fe(Tp)_2$ structure is not planar as drawn, but rather the six donor atoms from the two Tp molecules ligate the Fe center in an octahedral fashion. **C:** Experiments were conducted in the same KCl-K Phos buffer system used for ESR, and contained 0.4 mM NADPH and 30 nM of the TrxR variants. The reactions were started by the addition of $Fe(III)(Tp)_2$ to a final concentration of 50 μM, and the initial rates at 37°C (determined by the increase in absorbance at 610 nm) were taken from the linear portion during the first 20 s of the assay. The molar extinction coefficient of $Fe(II)(Tp)_2$ at 610 nm (3.73 mM^{-1} cm^{-1}) was used to calculate the rate per min per μM TrxR. The values shown are the mean ± S.D. for three independent experiments. In comparison to wtTrxR, *p<0.05, **p<0.01, ***p<0.001. The results for C59S are different from those for C59S/C64S (p<0.05). A representative experiment on which these rates are based is shown in Supplemental Fig. S4A.

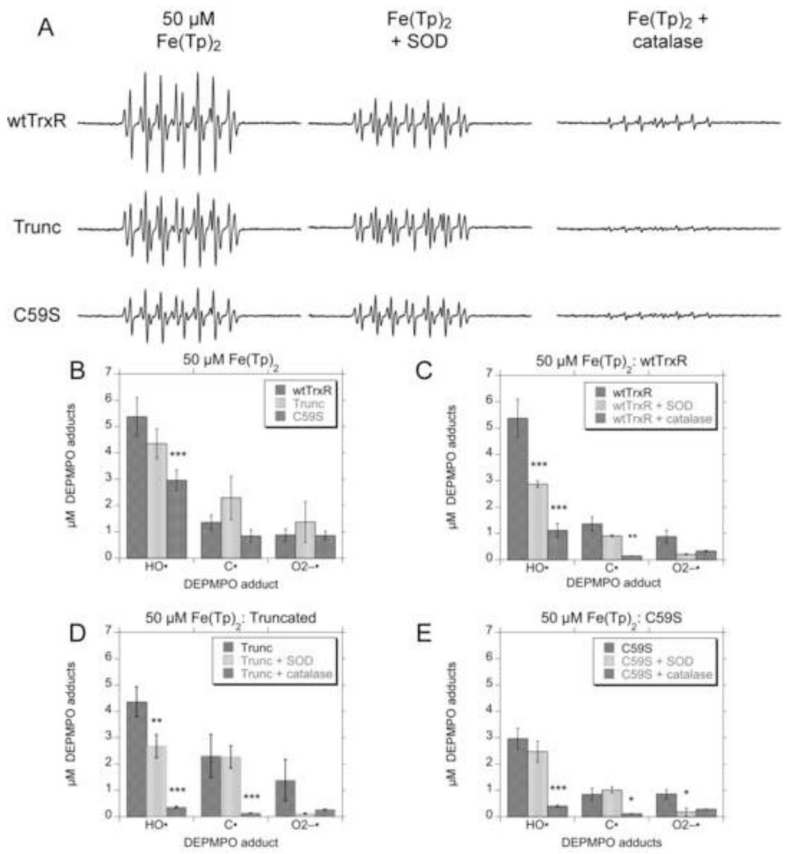

Fig. 5.

Radical generation with Fe(III)$(Tp)_2$ and wtTrxR, truncated TrxR, or the C59S variant. (A) Examples of ESR spectra for each DEPMPO adducts generated by the 3 TrxR variants. Samples were incubated for 15 min at 37°C under room air, and contained 14 mM DEPMPO, 0.4 mM NADPH, 50 μM Fe(III)$(Tp)_2$, and 0.3 μM of the indicated TrxR variant, and the effects of SOD (333 U ml^{-1}) or catalase (1666 U ml^{-1}) are also shown. (B) Quantification of the signal intensities for the DEPMPO adducts for wtTrxR and the truncated and C59S variants. In panels (C), (D), and (E), the effects of catalase and SOD on the DEPMPO adducts are quantified for wtTrxR (C), truncated TrxR (D), and the C59S variant (E). Panels B–E show the mean ± S.D. (n = 3) for each adduct. In (B), ***p<0.001 relative to the wtTrxR values. In panels (C) through (E), significant effects of catalase or SOD are indicated (*p<0.05; **p<0.01; ***p<0.001). See Fig. 1 for the ESR instrument settings.

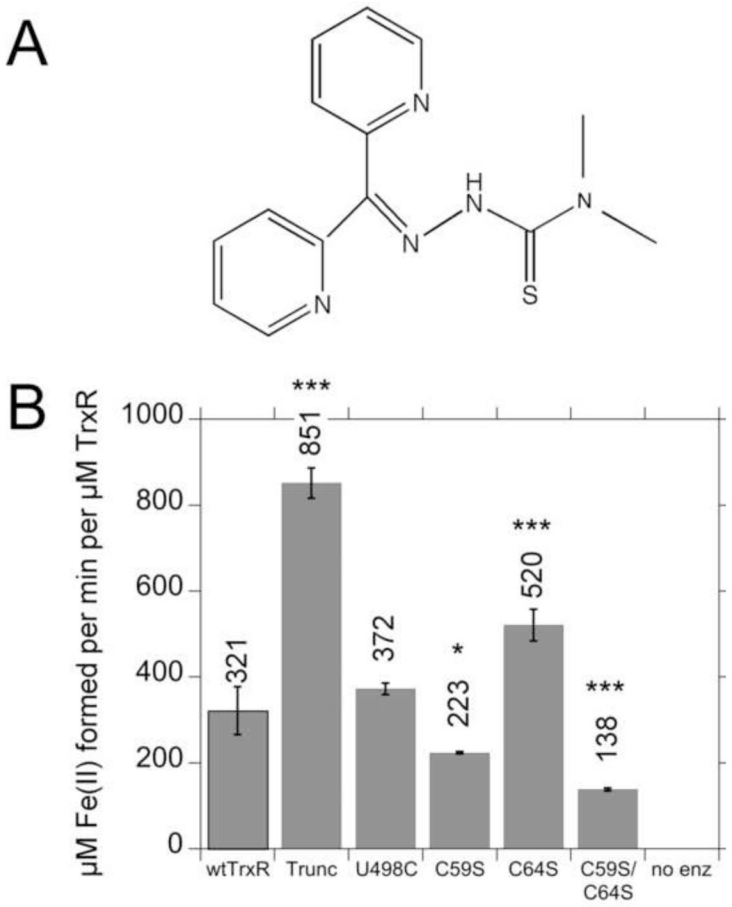

Fig. 6.

(A) Structure of Dp44mT, and (B) rates of reduction of Fe(III)(Dp44mT)$_2$ by wtTrxR and its site-directed variants. Experiments were conducted in the same KCl-K Phos buffer system used for ESR, and contained 0.4 mM NADPH and 30 nM of the TrxR variants. The reactions were started by the addition of Fe(III)(Dp44mT)$_2$ to a final concentration of 50 μM, and the initial rates at 37°C (determined by the increase in absorbance at 623 nm) were taken from the linear portion during the first 50 sec of the assay. The molar extinction coefficient of Fe(II)(Dp44mT)$_2$ at 623 nm (4.19 mM^{-1} cm^{-1}) was used to calculate the rate per min per μM TrxR. The values shown are the mean ± S.D. for three independent experiments. In comparison to wtTrxR, *p<0.05, ***p<0.001. The results for C59S are different from those for C59S/C64S (p<0.05). A representative experiment on which these rates are based is shown in Supplemental Fig. S4B.

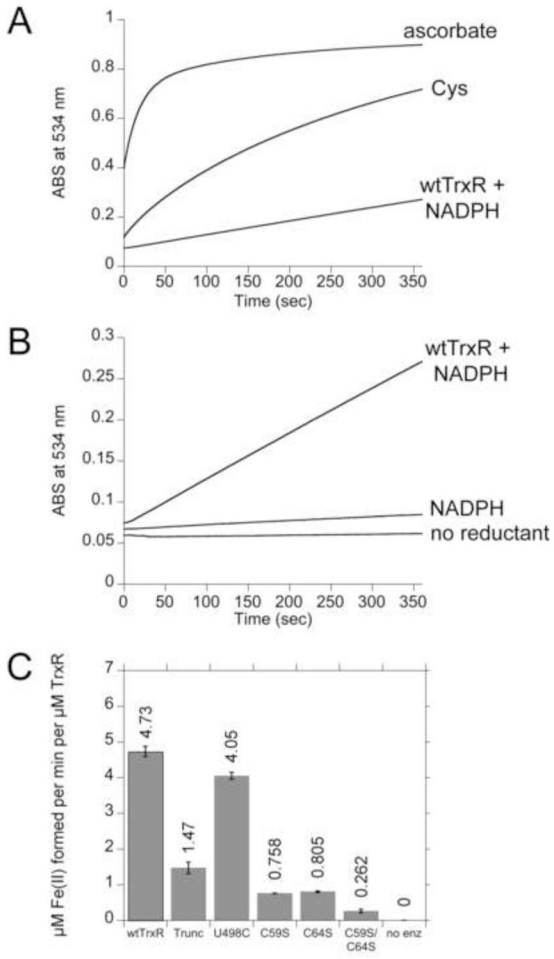

Fig. 7.

Representative experiments showing the rates of Fe(III)-Blm reduction by various reductants. All experiments included 50 μM Fe(III)-Blm and 1 mM BPS. BPS rapidly extracts the Fe(II) from Fe(II)-Blm, forming $Fe(II)(BPS)_3$ which was followed by increased absorbance at 534 nm. (A) The reactions were initiated by the addition of the reductants as indicated (0.2 mM ascorbate, 0.2 mM Cys, or 0.3 μM wtTrxR and 0.4 mM NADPH). (B) An expanded view showing the rate of Fe(III)-Blm reduction catalyzed by wtTrxR compared to NADPH alone or no reductant. (C) Rates of reduction of Fe(III)-Blm by wtTrxR and its site-directed variants. For C, the trace amounts of reduction catalyzed by NADPH alone were subtracted to determine the net rates for each TrxR variant.